PHYSICAL REVIEW A VOLUME 23, NUMBER 3 MARCH 1981

Frequency-dependent critical diffusion in a classical fluid

Jayanta K. Bhattacharjee and Richard A. Ferrell
Institute for Theoretical Physics, University of California, Santa Barbara, California 93106
and Center for Theoretical Physics, Department of Physics and Astronomy, University of Maryland, College Park, Maryland 20742
(Received 2 September 1980)

The frequency dependence of diffusion in a classical fluid is a consequence of the frequency dependence of the viscosity and leads to a small but observable deviation from a pure exponential decay of the order-parameter fluctuations. Our calculation of the deviation at the critical point gives a good fit to the data of Burstyn, Chang, and Sengers. The theory also agrees with the temperature dependence that they found.

I. INTRODUCTION

One of the major predictions of critical dynamics is the nonexponential decay of the time-dependent correlation functions for various types of fluctuations. The resulting non-Lorentzian spectral shape has been calculated for the entropy fluctuations in liquid helium near the lambda point,[1-3] for the magnetization and staggered magnetization fluctuations in the antiferromagnet near the Néel point,[4] and the magnetization fluctuations near the Curie point in an isotropic ferromagnet.[5] But this effect has not yet been treated theoretically for the classical fluids, doubtless because experimentally the small deviation from Lorentzian shape has until recently evaded detection. This is unfortunate as it might lead to the conclusion that the classical fluid constitutes an exception to the general rule that critical fluctuations have a non-Lorentzian spectrum. To show in detail that the classical fluid is not a special case apart, but in fact fits well into the general picture, is the motivation for our calculation in this paper of the deviation from exponential decay of the order-parameter correlation function. The order parameter is the entropy density and the concentration in the single- and two-component fluid, respectively. We demonstrate that, although small, the effect very definitely exists. Our calculations yield good agreement with the recent experiments of Burstyn, Chang, and Sengers[6] detecting this elusive effect.

The cause of the non-Lorentzian spectrum is the frequency-dependent diffusion coefficient. The reason that the effect is small and had hitherto been neglected is that the frequency dependence in the diffusion coefficient does not enter at $O(\epsilon)$ in an ϵ expansion about $D=4$. To calculate the effect one has to go to $O(\epsilon^2)$. In other words one has to consider the frequency dependence of the viscosity. The work of Kawasaki and Ohta[7] ignores this effect and consequently is not relevant in the critical region. Calculation of frequency dependence for any system to $O(\epsilon^2)$ in the different formulations of critical dynamics is a highly nontrivial task, which to our knowledge has not been performed. In this work, we will avoid these difficulties by working with the dressed single-loop diagrams[7] for the viscosity and diffusion coefficient. By working within a self-consistent scheme in $D=3$, we actually incorporate effects to all orders in ϵ. The two and higher loop diagrams will in principle contribute. But, for the classical fluid, the contribution of these diagrams is suppressed by a geometrical factor that is responsible for the small value of the viscosity exponent, and hence can be neglected. This is the same reason that the single-loop Kawasaki function is a good description of the wave number- and temperature-dependent relaxation rate.

The physical basis for the nonexponential decay rests, as mentioned above, with the frequency dependence of the critical viscosity. The divergent critical component of the latter disappears at high frequencies because the underlying fluctuations which are responsible for the critical viscosity cannot follow at frequencies higher than the characteristic relaxation rate of the fluid. As a consequence the short-time decay of an order-parameter fluctuation is determined by the noncritical background viscosity. But at later times the critical component of the viscosity sets in, resulting in a slower decay. A semi-logarithmic plot of the correlation function versus time will therefore show an upwards curvature. Our quantitative calculation of this curvature is based on a spectral-function approach. The frequency-dependent integral cannot be evaluated in closed form. Consequently, the spectral function has to be determined in an approximate manner. To establish the reliability of our spectral function we proceed in three steps.[8] The simplest spectral function, a step function, is considered first and yields answers in closed form. A slightly more sophisticated two-term spectral function is considered next and the answer can once again be expressed

in closed form. Finally, a three-term spectral function which we believe to be a very close approximation to the truth, is considered. Now the answers can no longer be expressed in terms of tabulated functions but can be obtained as series expansions. The differences between the answers with the three different spectral functions are moderate and systematic (see, for example, Fig. 4) and serve to establish the credibility of our approximations.

In Sec. II we establish the general formulas for the deviation of the time-dependent correlation function from the simple exponential form. In Sec. III the special case of the binary liquids is considered and a three-term high-frequency expansion for the diffusion coefficient is established. Section IV deals with the spectral function. The results at the critical point are shown and compared with the experiments of Burstyn, Chang, and Sengers[6] in Sec. V. The temperature dependence is discussed in Sec. VI. Section VII concludes with a brief summary.

II. FREQUENCY-DEPENDENT DIFFUSION

The intensity of the light scattered by a fluctuation of wave number k is proportional to $\chi(k,\kappa)$, the Fourier transform of the equal-time order-parameter correlation function. In this paper we will use throughout the Ornstein-Zernike approximation[9]

$$\chi(k,\kappa)=\frac{1}{k^2+\kappa^2}\,, \tag{2.1}$$

where κ^{-1} is the correlation length. This approximation is justified by the small value of the critical index η, which is known to amount to only a few percent.[10,11] The distribution of the scattered light in frequency ω is given by the Fourier transform of the time-dependent factor of the order-parameter correlation function,

$$g(k,\kappa,\omega)=\frac{1}{-i\omega+\gamma(k,\kappa,\omega)}\,. \tag{2.2}$$

The frequency-dependent rate, which is a kind of memory function, is given by

$$\gamma(k,\kappa,\omega)=\frac{k^2}{\chi(k,\kappa)}\,\lambda(k,\kappa,\omega)\,. \tag{2.3}$$

$\chi(k,\kappa)^{-1}$ is the thermodynamic stiffness of the system, while the final factor in the right-hand member of Eq. (2.3) is the critical Onsager coefficient. As is indicated by the dependence of this function on both k and ω, this function represents a nonlocal conductivity. The ratio λ/χ is a nonlocal diffusion coefficient. It is the purpose of this paper to explore the experimental consequences of the frequency dependence of λ, which reveals itself as a departure of the relaxation of the fluctuations from exponential decay.

The inverse Fourier transform of Eq. (2.2) is the time correlation function

$$G(k,\kappa,t)=\frac{1}{2\pi}\int_{-\infty}^{+\infty}d\omega\, g(k,\kappa,\omega)e^{-i\omega t}\,. \tag{2.4}$$

Because γ is a causal function, analytic in the upper half of the frequency plane, it follows that Eq. (2.4) vanishes for $t<0$. We further assume that γ is bounded in the entire lower half of the complex frequency plane. For $t>0$ this permits us to deform the contour of integration into a very large circle. γ can then be neglected in the denominator of Eq. (2.2) and we obtain the sum rule

$$G(k,\kappa,0+)=1\,. \tag{2.5}$$

The frequency dependence of the diffusion in a classical fluid is a very small effect. Therefore it is useful to take the $\omega=0$ value of γ as a reference value. To a first approximation the frequency dependence of γ can be neglected in the denominator of Eq. (2.2). Replacing γ by

$$\gamma_k\equiv\gamma(k,\kappa,0)\,, \tag{2.6}$$

leads to the simple exponential decay

$$G(k,\kappa,t)\simeq e^{-\gamma_k t}=e^{-\tau}\,. \tag{2.7}$$

Here we have introduced the dimensionless time variable $\tau=\gamma_k t$. In order to reveal the deviation from exponential decay we introduce the deviation function

$$\Delta G(k,\kappa,\tau)\equiv G(k,\kappa,t)-e^{-\tau}\,. \tag{2.8}$$

The sum rule of Eq. (2.5) becomes now

$$\Delta G(k,\kappa,0+)=0\,. \tag{2.9}$$

We can obtain a second sum rule by integrating over the deviation function. This gives the zero-frequency Fourier component

$$\int_0^\infty d\tau\,\Delta G(k,\kappa,\tau)=\frac{\gamma_k}{\gamma(k,\kappa,0)}-1=0\,, \tag{2.10}$$

by virtue of Eq. (2.6). It follows that ΔG must have at least one zero.

The deviation from exponential decay is evident as a nonlinearity in the plot of $\ln G$ vs τ. In terms of the deviation function this is

$$\begin{aligned}\ln G&=\ln(e^{-\tau}+\Delta G)=-\tau+\ln(1+e^{\tau}\Delta G)\\&\simeq-\tau+e^{\tau}\Delta G\,,\end{aligned} \tag{2.11}$$

where the expansion of the logarithm is justified

for $\tau = O(1)$ by $|\Delta G| \ll 1$. Taking the derivative helps to reveal the underlying small frequency-dependent effect. This yields, upon introducing the dimensionless frequency

$$\Omega = \omega/\gamma_k , \tag{2.12}$$

and the dimensionless deviation rate

$$\Gamma = [\gamma(k, \kappa, \omega) - \gamma_k]/\gamma_k , \tag{2.13}$$

$$\frac{d}{d\tau}(e^{\tau}\Delta G) = \frac{1}{2\pi}\int_{-\infty}^{+\infty} d\Omega \left(\frac{-i\Omega+1}{-i\Omega+1+\Gamma} - 1\right) e^{(-i\Omega+1)\tau}$$

$$\simeq -\frac{1}{2\pi}\int_{-\infty}^{+\infty} \frac{d\Omega}{-i\Omega+1}\,\Gamma e^{(-i\Omega+1)\tau} , \tag{2.14}$$

where to first order we are permitted to neglect Γ in the denominator of the integrand. A further differentiation gives the curvature function

$$\frac{d^2}{d\tau^2}(e^{\tau}\Delta G) = -e^{\tau}\frac{1}{2\pi}\int_{-\infty}^{+\infty} d\Omega\,\Gamma(\Omega)e^{-i\Omega\tau} . \tag{2.15}$$

Except for the factor of $-\exp\tau$, this is nothing other than the inverse Fourier transform of the frequency-dependent relaxation rate. It is generally difficult to carry out the Fourier integration such as indicated in Eq. (2.15), and the problem is often more tractable when converted into a Laplace integration. This is the case here because, as will be established in the subsequent section, the analytic properties of the relaxation rate are especially simple. The singularities lie entirely along a cut on the negative imaginary axis. We therefore change to the variable

$$s = i\Omega , \tag{2.16}$$

and deform the contour of integration into a loop along the cut to find (with the k and κ dependence no longer being exhibited explicitly)

$$\frac{d^2}{d\tau^2}(e^{\tau}\Delta G) = -\frac{1}{\pi}\int_{s_0}^{\infty} ds\,\mathrm{Im}\Gamma(-is+\delta)e^{(1-s)\tau} . \tag{2.17}$$

δ is a positive infinitessimal quantity, ensuring that the imaginary part of Γ is evaluated along the right-hand side of the cut, beginning at the branch point, or threshold, at $s = s_0$.

Integration of Eq. (2.17) with respect to τ within the integrand yields a Laplace transform for the slope function. This is in the form, however, of an improper integral with an inadequately defined singularity at $s = 1$. Therefore it is preferable to return to the Fourier transform for the slope function and to carry out the deformation of the contour of integration on Eq. (2.14). Upon doing this, we find a distributed contribution from the cut and a discrete contribution from the pole at $\Omega = -i$. Only $\mathrm{Re}\Gamma$ contributes to the residue at the pole. The distributed contribution is a Cauchy principal value integral. Thus we obtain

$$\frac{d}{d\tau}(e^{\tau}\Delta G) = -\mathrm{Re}\Gamma(-i) + \frac{1}{\pi}\,\mathrm{P}\int_{s_0}^{\infty}\frac{ds}{s-1}\,\mathrm{Im}\Gamma e^{(1-s)\tau} . \tag{2.18}$$

A further integration using the sum rule of Eq. (2.9) as an initial condition gives

$$\Delta G = -\mathrm{Re}\Gamma(-i)\tau e^{-\tau} + \frac{1}{\pi}\,\mathrm{P}\int_{s_0}^{\infty}\frac{ds}{(s-1)^2}\,\mathrm{Im}\Gamma(e^{-\tau} - e^{-s\tau}) . \tag{2.19}$$

It is worthwhile to verify that Eq. (2.19) satisfies the sum rules. The zero-time sum rule is satisfied identically. We therefore turn to the zero-frequency component which, according to Eq. (2.19), is

$$\int_0^{\infty}\Delta G\,d\tau = -\mathrm{Re}\Gamma(-i) + \frac{1}{\pi}\,\mathrm{P}\int_{s_0}^{\infty}\frac{ds}{s(s-1)}\,\mathrm{Im}\Gamma . \tag{2.20}$$

In order to verify that the two terms of Eq. (2.20) cancel, as required by the sum rule of Eq. (2.10), we need a dispersion relation for Γ. Cauchy's theorem in subtracted form, with the subtraction point at $\Omega = 0$, reads

$$\Gamma(\Omega) = \frac{1}{2\pi i}\oint d\Omega'\left(\frac{1}{\Omega'-\Omega} - \frac{1}{\Omega'}\right)\Gamma(\Omega')$$

$$= \frac{i\Omega}{\pi}\int_{s_0}^{\infty}\frac{ds}{s(s-i\Omega)}\,\mathrm{Im}\Gamma . \tag{2.21}$$

Evaluated at the pole this gives

$$\mathrm{Re}\Gamma(-i) = \frac{1}{\pi}\,\mathrm{P}\int_{s_0}^{\infty}\frac{ds}{s(s-1)}\,\mathrm{Im}\Gamma , \tag{2.22}$$

resulting in the required cancellation.

$\mathrm{Re}\Gamma(-i)$ is the amount by which the pole is shifted because of the frequency dependence. The first term of Eq. (2.19) combines with the zero-order expression for G to give the exponential decay

$$e^{-\tau}[1 - \mathrm{Re}\Gamma(-i)\tau] \simeq e^{-\tau}\exp[-\mathrm{Re}\Gamma(-i)\tau]$$

$$= \exp-[1 + \mathrm{Re}\Gamma(-i)]\tau \tag{2.23}$$

at the modified rate $1 + \mathrm{Re}\Gamma(-i)$. The corresponding strength renormalization constant for the pole, using Eq. (2.21), is given by

$$Z^{-1}-1=i\frac{\partial}{\partial\Omega}\,\mathrm{Re}\Gamma\Big|_{\Omega=-i}$$
$$=-\frac{1}{\pi}\,\mathrm{P}\int_{s_0}^{\infty}\frac{ds}{s-1}\frac{d\,\mathrm{Im}\Gamma}{ds}\,. \tag{2.24}$$

The derivative at an arbitrary value of Ω along the cut is

$$i\frac{\partial}{\partial\Omega}\,\mathrm{Re}\Gamma=-\frac{1}{\pi}\,\mathrm{P}\int_{s_0}^{\infty}\frac{ds}{s-i\Omega}\frac{d\,\mathrm{Im}\Gamma}{ds}\,. \tag{2.25}$$

Only when Ω moves upwards along the negative imaginary axis above the branch point do we have $i\Omega<s_0$. The principal value sign can then be dropped and integration by parts carried out to yield

$$i\frac{\partial}{\partial\Omega}\,\mathrm{Re}\Gamma=-\frac{1}{\pi}\int_{s_0}^{\infty}\frac{ds}{(s-i\Omega)^2}\,\mathrm{Im}\Gamma\,. \tag{2.26}$$

If the pole were isolated from the cut, so that $s_0>1$, then we could substitute Eq. (2.26) into Eq. (2.24) to find

$$Z\simeq 1+\frac{1}{\pi}\int_{s_0}^{\infty}\frac{ds}{(s-1)^2}\,\mathrm{Im}\Gamma\,. \tag{2.27}$$

The $\tau\gg 1$ behavior of the correlation function would then be determined entirely by the pole renormalization parameters as

$$\Delta G=Ze^{-[1+\mathrm{Re}\Gamma(-i)]\tau}-e^{-\tau}$$
$$\simeq-\mathrm{Re}\Gamma(-i)\tau e^{-\tau}+\frac{e^{-\tau}}{\pi}\int_{s_0}^{\infty}\frac{ds}{(s-1)^2}\,\mathrm{Im}\Gamma\,. \tag{2.28}$$

Here we have substituted from Eqs. (2.23) and (2.27) and expanded only to first order in the small terms. Equation (2.28) is identical to Eq. (2.19) under the assumed conditions $s_0>1$ and $\tau\gg 1$ because in this case the second term in parentheses in the integrand of Eq. (2.19) is negligibly small compared to the first.

But the renormalization of the pole parameters do not, in fact, play an important role in the present work because, as we shall see in the next section, $s_0<1$ and the pole is *not* isolated from the cut. Therefore the pole contribution is not clearly separable from the contributions to the correlation function coming from the continuous distribution of spectral strength. We will consequently have no further use for Eq. (2.24) in this paper. Instead of Eq. (2.24), a more useful derivative is the initial slope. From Eqs. (2.26) and (2.25) we have

$$i\Gamma'(0)=-\frac{1}{\pi}\int_{s_0}^{\infty}\frac{ds}{s^2}\,\mathrm{Im}\Gamma=-\frac{1}{\pi}\int_{s_0}^{\infty}\frac{ds}{s}\frac{d\,\mathrm{Im}\Gamma}{ds}$$
$$=-\pi^{-1}\,\mathrm{Im}\Gamma(-i\infty+\delta)\langle s^{-1}\rangle, \tag{2.29}$$

where the "first moment" is defined by the average

$$\left\langle\frac{1}{s}\right\rangle=\frac{\displaystyle\int_{s_0}^{\infty}\frac{ds}{s}\frac{d\,\mathrm{Im}\Gamma}{ds}}{\displaystyle\int_{s_0}^{\infty}ds\,\frac{d\,\mathrm{Im}\Gamma}{ds}}\,. \tag{2.30}$$

Because the first moment is one of our main mathematical tools, it is useful also to have it expressed in terms of a mean time. We obtain such a relation from the Fourier transform of the deviation function [by substitution of Eq. (2.13)]

$$\Delta g(\Omega)=\int d\tau\, e^{i\Omega\tau}\Delta G(\tau)=\frac{-\Gamma(\Omega)}{(1-i\Omega)^2}\,. \tag{2.31}$$

Equation (2.31) differs from the subtracted version of Eq. (2.2) by a factor of γ_k. By differentiation within the integral and by virtue of $\Gamma(0)=0$ we obtain from Eq. (2.31)

$$i\Gamma'(0)=\int_0^{\infty}d\tau\,\tau\Delta G(\tau)\,. \tag{2.32}$$

Substitution from Eq. (2.29) yields therefore

$$\left\langle\frac{1}{s}\right\rangle=\frac{\displaystyle\int_{s_0}^{\infty}d\tau\,\tau\Delta G(\tau)}{-\pi^{-1}\,\mathrm{Im}\Gamma(-i\infty+\delta)}\,. \tag{2.33}$$

III. DECOUPLED-MODE THEORY

The decoupled-mode[12] version of critical dynamics is the lowest order in a systematic mode-coupling formalism based on the equations of motion. Because of the small effect being studied here, this lowest order version will be adequate for our purposes. In its simplest form it is based on the Kubo[13,14] formula for the transport coefficient responsible for the critical diffusion. The current which produces the transport of concentration in the binary liquid, or the transport of heat in the single-component liquid, is the product of the hydrodynamic shear velocity field and the scalar order parameter

$$J=v\phi\,. \tag{3.1}$$

For the Kubo formula we need the space-time correlation function of the current, which in its decoupled, or factorized, form is

$$\langle J(1)J(2)\rangle\simeq\langle v(1)v(2)\rangle\,\langle\phi(1)\phi(2)\rangle\,. \tag{3.2}$$

The Fourier component of the velocity correlation function at wave number p' and frequency ω' is

$$\langle v(1)v(2)\rangle_{p',\omega'} \simeq \frac{1}{-i\omega' + p'^2\eta(p', \kappa, \omega')} \simeq \frac{1}{p'^2\eta(p', \kappa, \omega')} . \quad (3.3)$$

The approximation in the final expression is justified by the critical slowing down. The diffusion rate is consequently very small compared to the damping rate of the shear modes. The hydrodynamic shear viscosity has the critical variation

$$\eta(0, \kappa, 0) \propto \kappa^{-z_\eta} , \quad (3.4)$$

where the critical index from decoupled-mode theory is

$$z_\eta = \frac{8}{15\pi^2} = 0.054 . \quad (3.5)$$

The renormalization group to two-loop order in the ϵ expansion (where the space dimensionality is $D = 4 - \epsilon$) gives the slightly larger number[15]

$$z_\eta = 0.065 . \quad (3.6)$$

It follows from scaling that the wave-number dependence of the viscosity at the critical point is

$$\eta(k, 0, 0) \propto k^{-z_\eta} . \quad (3.7)$$

Similarly, scaling requires the viscosity in the long wavelength limit to have the critical point frequency dependence

$$\eta(0, 0, \omega) \propto (-i\omega)^{-z_\eta/3} , \quad (3.8)$$

where we are neglecting a small correction to the exponent of $O(z_\eta^2)$.

For the rest of this section, in the interest of simplicity, we will work exactly at the critical point, where $\kappa = 0$. The temperature dependence will be taken up in Section VI. For the present purposes we need the scaling function of the variables k and ω which will bridge between the two limiting cases expressed by Eqs. (3.7) and (3.8) above. This function has been computed by Perl and Ferrell[16] and plotted as their Fig. 3. A convenient alternative is the lowest order four-dimensional expansion result of the present authors,[17]

$$\eta(k, 0\omega) = \eta(k, 0, 0)[1 - iA(\omega/\gamma_k)]^{-z_\eta/3} \simeq \eta(k, 0, 0)\{1 - \tfrac{1}{3}z_\eta \ln[1 - iA(\omega/\gamma_k)]\}, \quad (3.9)$$

where

$$A = 3\pi - 6 - 6\ln 2 = 0.734 . \quad (3.10)$$

This provides an excellent overall fit to the Perl-Ferrell[16] curve. The value of A is in fact a compromise between the values of 0.95 and 0.60 which give low- and high-frequency fits, respectively, to the Perl-Ferrell curve. The expansion of the exponential of the power in its logarithmic form is permitted by $z_\eta \ll 1$. The computation of the frequency dependent decay rate requires the reciprocal of the viscosity which again, because of $z_\eta \ll 1$, can be written as

$$\eta(k, 0, \omega)^{-1} \simeq \eta(k, 0, 0)^{-1}\{1 + \tfrac{1}{3}z_\eta \ln[1 - iA(\omega/\gamma_k)]\} . \quad (3.11)$$

The diffusion rate $\gamma(k, 0, \omega)$ is determined by the k, ω Fourier component of Eq. (3.2). The product of the correlation functions thereby becomes a convolution integral over the wave numbers $\vec{p}'$ and $\vec{p}$ constrained by momentum conservation

$$\vec{p} + \vec{p}' = \vec{k} . \quad (3.12)$$

The $\vec{p}$ component of the order-parameter correlation function decays as $\exp(-\gamma_p t)$, corresponding to frequency $-i\gamma_p$. "Frequency conservation" therefore requires

$$-i\gamma_p + \omega' = \omega . \quad (3.13)$$

This causes the logarithmic term in Eq. (3.11) to become

$$\ln\left(1 - iA\frac{\omega'}{\gamma_{p'}}\right) = \ln\left(1 + A\frac{\gamma_p}{\gamma_{p'}} - A\frac{i\omega}{\gamma_{p'}}\right) = \ln\left(1 + A\frac{\gamma_p}{\gamma_{p'}}\right) + \ln\left(1 - \frac{iA\omega}{A\gamma_p + \gamma_{p'}}\right) = \ln\left(1 + A\frac{\gamma_p}{\gamma_{p'}}\right) + \ln\left(1 - i\frac{\gamma_k\Omega}{\gamma_p + A^{-1}\gamma_{p'}}\right) , \quad (3.14)$$

where the dimensionless frequency has been introduced from Eq. (2.12). The effect of the first term of Eq. (3.14) on $\eta(k, 0, 0)$ has been studied by Perl and Ferrell[16] and will not be discussed further here. We are interested now in the net frequency dependence resulting from the second term when the p, p' values are weighted according to the convolution integration. At this point it is convenient to scale the intermediate wave numbers with respect to the external wave number, so that Eq. (3.12) becomes $\vec{p} + \vec{p}' = \vec{k}/k$, of unit magnitude. Because γ_k varies as k to the power[18] $3 + z_\eta \simeq 3$, the coefficient of $-i\Omega$ in Eq. (3.14) becomes $(p^3 + A^{-1}p'^3)^{-1}$. With these preliminaries

out of the way we can now substitute Eqs. (3.14) and (3.11) into Eqs. (3.3), (3.2), and (2.13) to obtain

$$\Gamma(\Omega)=\frac{z_\eta}{3}\tilde{\Gamma}(\Omega)$$
$$=\frac{z_\eta}{3}\left\langle \ln\left(1-i\frac{\Omega}{p^3+A^{-1}p'^3}\right)\right\rangle . \quad (3.15)$$

By virtue of the subtraction at zero frequency, from now on all quantities of interest will carry the small coefficient $z_\eta/3=0.065/3=0.0217$. We therefore simplify the notation by omitting this coefficient and distinguishing the resulting quantity by a tilde. The average of a quantity L is defined by the integral

$$\langle L\rangle = I^{-1}\frac{1}{4\pi}\int\frac{d^3p'}{p^2p'^2}\sin^2\theta' L , \quad (3.16)$$

where θ' is the angle between $\vec{p}'$ and $\vec{k}$. The normalizing integral is the decoupled-mode expression to zero order,

$$I=\frac{1}{4\pi}\int\frac{d^3p'}{p^2p'^2}\sin^2\theta'=\frac{\pi^2}{8} . \quad (3.17)$$

It will be noted that $z_\eta \ll 1$ has permitted us to neglect the viscosity in Eqs. (3.16) and (3.17).

According to Eq. (3.15) the initial slope is

$$i\tilde{\Gamma}'(0)=\left\langle\frac{1}{p^3+A^{-1}p'^3}\right\rangle . \quad (3.18)$$

From Eq. (3.15) we see that the coefficient in the right-hand member of Eq. (2.29) is

$$-\pi^{-1}\mathrm{Im}\Gamma(-i\infty+\delta)=z_\eta/3 .$$

Comparison of Eq. (3.18) with Eq. (2.29) consequently permits us to identify the quantity within angular brackets in Eq. (3.18) with the first moment defined by Eq. (2.30). In the next section we will establish the full equivalence of the averages defined in these two different ways.

The inverse moment provides useful information. The integration in Eq. (3.18) can be carried out in bipolar (elliptic) coordinates, as in the computations of Perl and Ferrell,[16] if we depart from Eq. (3.10) and set $A=1.0$. For this special case the integration is done analytically in Appendix A, yielding

$$\langle(p^3+p'^3)^{-1}\rangle=0.520 . \quad (3.19)$$

The choice of $A=1.0$, although "unphysical" in that it is in conflict with Eq. (3.10), is a convenient mathematical simplification which will be used in the next section for studying certain properties of the spectral function. The deviation of the first moment from Eq. (3.19) for $A=1+\Delta A$, to first order in ΔA, can be estimated from

$$\left\langle\frac{1}{p^3+A^{-1}p'^3}\right\rangle=\left\langle\frac{A^{1/2}}{A^{1/2}p^3+A^{-1/2}p'^3}\right\rangle$$
$$\simeq(1+\tfrac{1}{2}\Delta A)\langle[p^3+p'^3+\tfrac{1}{2}\Delta A(p^3-p'^3)]^{-1}\rangle$$
$$\simeq(1+\tfrac{1}{2}\Delta A)\left\langle(p^3+p'^3)^{-1}\left(1-\tfrac{1}{2}\Delta A\frac{p^3-p'^3}{p^3+p'^3}\right)\right\rangle$$
$$=[1+(1-\beta)\tfrac{1}{2}\Delta A]\langle(p^3+p'^3)^{-1}\rangle , \quad (3.20)$$

where

$$0<\beta<1 . \quad (3.21)$$

β is a kind of average value of $(p^3-p'^3)/(p^3+p'^3)$. The inequality follows from the asymmetry introduced into the integrals of Eqs. (3.16) and (3.17) by $\sin^2\theta'$. This factor tends to suppress the contributions from momentum space where $p'>p$. As the upper limit corresponds to the point $p'=0$, of zero measure, we may fairly estimate $\beta\simeq\frac{1}{3}\pm\frac{1}{3}$, so the fractional reduction in the first moment is given by

$$\langle(p^3+A^{-1}p'^3)^{-1}\rangle\simeq[1+(1.0\pm0.5)\tfrac{1}{3}\Delta A]\langle(p^3+p'^3)^{-1}\rangle . \quad (3.22)$$

With $\Delta A=-0.27$ from Eq. (3.10) we find a fractional reduction of $9\pm5\%$, which changes Eq. (3.19) into

$$\langle(p^3+A^{-1}p'^3)^{-1}\rangle\simeq0.47\pm0.03 . \quad (3.23)$$

In order to carry out the averaging in wave-number space required by Eq. (3.16), it is necessary to find a means of doing the integration for arbitrary values of Ω. This is in general a difficult task. We have, however, found that a high-frequency expansion provides a great simplification and yields satisfactory results. In the range $\Omega\gg1$ we can write the logarithm in Eq. (3.15) in the form

$$\ln\left(1-i\frac{\Omega}{p^3+A^{-1}p'^3}\right)=\ln\frac{-i\Omega}{p^3+A^{-1}p'^3}+\ln\left(1+\frac{p^3+A^{-1}p'^3}{-i\Omega}\right) . \quad (3.24)$$

Thus the leading term in the average of Eq. (3.24) is $\ln(-i\Omega)$ and requires no integration. The corrections to the leading term are given by

$$\tilde{\Gamma}(\Omega)=\ln(-i\Omega)-\langle\ln(p^3+A^{-1}p'^3)+\left\langle\ln\left(1+\frac{p^3+A^{-1}p'^3}{-i\Omega}\right)\right\rangle . \quad (3.25)$$

The constant correction to the logarithm has been calculated by Perl and Ferrell[16] using a two-step procedure and was found to be equal to -2.11. As they did not use an approximation for the viscosity of the form of Eq. (3.9), their numerical result cannot be put directly into the present framework. However, to the accuracy with which Eq. (3.9) is a good fit, we can use their result to write

$$\langle \ln(p^3 + A^{-1}p'^3)\rangle = 2.11\,, \tag{3.26}$$

where A is given by Eq. (3.10). In the next section we find from our own calculation

$$\langle \ln(p^3 + A^{-1}p'^3)\rangle = 2.14\,,$$

in confirmation of Eq, (3.26) and the underlying approximations. The inequality

$$\langle \ln(p^3 + A^{-1}p'^3)\rangle \geq \ln\left\langle \frac{1}{p^3 + A^{-1}p'^3}\right\rangle^{-1} \tag{3.27}$$

follows from the convexity of the logarithm and is evidently satisfied by Eqs. (3.26) and (3.23).

The calculation of the frequency-dependent correction term in Eq. (3.25) is easily carried out to lowest order. By virtue of $\Omega \gg 1$ the dominant contributions in p space come from the range $p \simeq p' \gg 1$. The distinction between p and p' can therefore be neglected, which reduces the convolution integral to

$$\left\langle \ln\left(1 + \frac{p^3 + A^{-1}p'^3}{-i\Omega}\right)\right\rangle \simeq \left\langle \ln\left(1 + \frac{1 + A^{-1}}{-i\Omega}\, p^3\right)\right\rangle$$
$$\simeq \frac{2}{3I}\int_0^\infty \frac{dp}{p^2} \ln\left(1 + \frac{1 + A^{-1}}{-i\Omega}\, p^3\right) = \frac{2}{9I}\left(\frac{1 + A^{-1}}{-i\Omega}\right)^{1/3} \int_0^\infty \frac{du}{u^{4/3}} \ln(1 + u)\,. \tag{3.28}$$

(The angular average of $\sin^2\theta'$ is $\frac{2}{3}$.) The definite integral is equal to $3\pi/\sin(\pi/3)$ so that substituting this and the value of I from Eq. (3.17) gives

$$\left\langle \ln\left(1 + \frac{1 + A^{-1}}{-i\Omega}\, p^3\right)\right\rangle \simeq \frac{32}{3\pi\sqrt{3}}\left(\frac{1 + A^{-1}}{-i\Omega}\right)^{1/3}\,. \tag{3.29}$$

A further term in the high-frequency expansion for $\Gamma(\Omega)$ is obtained by calculating the error in the high-momentum approximation used above. This error will accumulate over the entire interval $1 \lesssim p' \lesssim (-i\Omega)^{1/3}$, where we will now have to pay attention to the slight difference between p and p'. The error incurred in the approximation $p = p'$ is found by keeping $p^3 + A^{-1}p'^3$ unaltered as well as by introducing a correction factor p'^2/p^2 in the integrand. (The latter changes the weighting function from the high-momentum approximation of p'^{-4} back to its original form where p is not equated to p'.) The correction to the previous work is consequently

$$\Delta\left\langle \ln\left(1 + \frac{p^3 + A^{-1}p'^3}{-i\Omega}\right)\right\rangle \simeq \frac{1}{-i\Omega}\,\Delta\langle (p^3 + A^{-1}p'^3)\rangle$$
$$= \frac{1}{-i\Omega}\left\langle \frac{p'^2}{p^2}\,(p^3 + A^{-1}p'^3) - (1 + A^{-1})p'^3\right\rangle$$
$$= \frac{1}{-i\Omega}\,\langle p'^2(p - p')\rangle + \frac{A^{-1}}{-i\Omega}\left\langle p'^5\left(\frac{1}{p^2} - \frac{1}{p'^2}\right)\right\rangle\,. \tag{3.30}$$

We obtain the required averages by substituting

$$p^2 = 1 + p'^2 + 2p'\cos\theta'\,. \tag{3.31}$$

Taking advantage of $p' \gg 1$, we have for the difference of the two variables

$$p - p' \simeq \frac{1}{2p'}\,(1 - \cos^2\theta') + \cos\theta'$$
$$\Rightarrow \frac{1}{2p'}\,(1 - \langle\cos^2\theta'\rangle) = \frac{1}{2p'}\,(1 - \tfrac{1}{5}) = \frac{2}{5p'}\,, \tag{3.32}$$

where the second line expresses the result of angle averaging (with the weighting factor $\sin^2\theta'$). The other difference required in Eq. (3.24) is

$$\frac{1}{p^2}-\frac{1}{p'^2}\simeq-\frac{1-4\cos^2\theta'}{p'^4}-2\frac{\cos\theta'}{p'^3}$$

$$\Rightarrow -\frac{1}{p'^4}\left(1-\tfrac{4}{5}\right)=-\frac{1}{5p'^4}\,. \tag{3.33}$$

Substituted into Eq. (3.30), Eqs. (3.33) and (3.32) tend to cancel one another, yielding

$$\Delta\left\langle\ln\left(1+\frac{p^3+A^{-1}p'^3}{-i\Omega}\right)\right\rangle=\frac{1}{-i\Omega}\frac{2-A^{-1}}{5}\langle p'\rangle$$

$$=\frac{1}{-i\Omega}\frac{4-2A^{-1}}{15I}\int\frac{dp'}{p'}\simeq\frac{4-2A^{-1}}{15I}\frac{\ln(-i\Omega)^{1/3}}{-i\Omega}=\frac{16(2-A^{-1})}{45\pi^2}\frac{\ln(-i\Omega)}{-i\Omega} \tag{3.34}$$

to logarithmic accuracy. The divergent integral is naturally cut off below at $p'\simeq 1$. The upper cutoff is determined by the breakdown of the approximation used in the first step of Eq. (3.30) (the expansion of the logarithm). Therefore, the upper limit of the integral is $(-i\Omega)^{1/3}$. Substituting Eqs. (3.34) and (3.29) into Eq. (3.25) gives the four-term high-frequency approximation

$$\tilde{\Gamma}(\Omega)=\ln(-i\Omega)-\langle\ln(p^3+A^{-1}p'^3)\rangle+\frac{32}{3\pi\sqrt{3}}\left(\frac{1+A^{-1}}{-i\Omega}\right)^{1/3}+\frac{16(2-A^{-1})}{45\pi^2}\frac{\ln(-i\Omega)}{-i\Omega}\,. \tag{3.35}$$

IV. SPECTRAL FUNCTION

It is convenient to express the analytic continuation of $\Gamma(\Omega)$ to the right-hand side of the cut, which is required for the various expressions in Sec. II, in terms of a spectral function $f(s)$ defined by

$$\mathrm{Im}\,\tilde{\Gamma}(-is+\delta)=-\pi f(s)\,. \tag{4.1}$$

According to Eq. (3.35) the three-term high-frequency approximant for the spectral function is

$$f(s)=1-as^{-1/3}-bs^{-1}\,, \tag{4.2}$$

where

$$a=\frac{16}{3\pi^2}(1+A^{-1})^{1/3} \tag{4.3}$$

and

$$b=\frac{16}{45\pi^2}(2-A^{-1})\,. \tag{4.4}$$

In order to make use of Eq. (4.2), we need to have some information on the range of validity of the high-frequency approximation. In other words, down to how small a value of s can Eq. (4.2) be used? This question will be studied in this section, by establishing and exploiting the positive definiteness and monotonicity of $-\mathrm{Im}\,\Gamma$. The basic idea is illustrated by the solid curve of Fig. 1, where we have plotted a three-term expression of the type of Eq. (4.2) vs s. It will be noted that $f(s)$ has a zero at $s=s_0=0.57$. For $s<s_0$, $f(s)$ would become negative. This is not permitted by the positive definiteness of the spectral function which we now proceed to establish.

We need to return to Eq. (3.15) and study the analytic continuation of the logarithm. At the cut this becomes

$$\mathrm{Im}\ln\left(1-i\frac{-is+\delta}{p^3+A^{-1}p'^3}\right)=-\pi\Theta(s-p^3-A^{-1}p'^3)\,, \tag{4.5}$$

where the step function is

$$\Theta(x)=\begin{cases}0, & x<0\\ 1, & x>0\,.\end{cases} \tag{4.6}$$

Substituting Eqs. (4.5) and (3.15) into Eq. (4.1) gives

$$f(s)=\langle\Theta(s-p^3-A^{-1}p'^3\rangle\,. \tag{4.7}$$

The positive definiteness of $f(s)$ follows from that of the step function. Furthermore, every increase in s adds a non-negative quantity to $f(s)$ so that, according to Eq. (4.7), the spectral function is also monotonically increasing. Additionally we see that $f(\infty)=1$ because in this limit the step

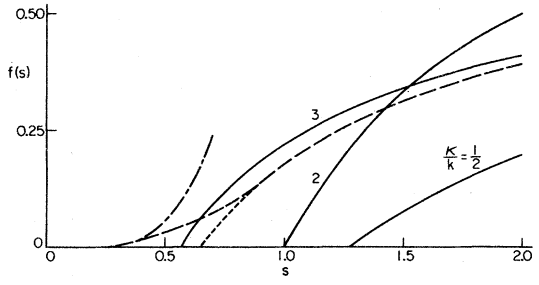

FIG. 1. Spectral function $f(s)$ versus frequency variable $s=i\Omega$. The threshold spectral function of Appendix C is shown by the dot-dash curve, while the dashed curve indicates the interpolating function between the physical threshold and the high-frequency approximant. The solid curves labeled 2 and 3 show the two- and three-term approximants, respectively. The shifted solid curve labeled $\kappa/k=\frac{1}{2}$ shows the three-term approximant at an elevated temperature.

function becomes identically equal to 1. For some purposes it is convenient to consider the derivative, which converts the step function into the Dirac delta function according to

$$f'(s) = \langle \delta(s - p^3 - A^{-1}p'^3) \rangle . \tag{4.8}$$

A simple application of Eq. (4.8) is to the first high-frequency correction term in the asymptotic behavior of $f(s)$. As in the derivation of Eq. (3.28), we can approximate $p \simeq p'$ and immediately carry out the angle averaging to find

$$\begin{aligned} f'(s) &= \frac{2}{3I} \int \frac{dp}{p^2} \delta(s - Bp^3) \\ &= \frac{2(B)^{1/3}}{9I} \int \frac{d(Bp^3)}{(Bp^3)^{4/3}} \delta(Bp^3 - s) \\ &= \frac{2(B)^{1/3}}{9I} s^{-4/3} , \end{aligned} \tag{4.9}$$

where $B = 1 + A^{-1}$. Integration of this expression with respect to s and substituting Eq. (3.17) reproduces the second term of the right-hand member of Eq. (4.2), with the coefficient in agreement with Eq. (4.3). In Appendix B we obtain the third term of Eq. (4.2) in a similar fashion.

The alternative derivation of the three-term spectral function provided by Eq. (4.9) and Appendix B makes it clear that Eq. (4.2) is subject to the general constraints of positivity and monotonicity. Therefore Eq. (4.2) must not be used for $s < s_0$. Thus we arrive at the picture of $f(s)$ vanishing for s less than some threshold value, and rising monotonically for s above threshold. Because of the error incurred in the high-frequency approximations the true threshold value will not necessarily equal s_0. This comparison can be made explicitly for the special case $A = 1$. Then the minimum value of $p^3 + p'^3$ occurs for $p = p' = \frac{1}{2}$, so the true threshold falls at the relatively small value of $s = \frac{1}{4}$. In Appendix C we demonstrate that the threshold behavior of $f(s)$ is proportional to $(s - \frac{1}{4})^{5/2}$. This rise at threshold is shown by the dot-dash curve in Fig. 1. The solid curve represents Eq. (4.2) with b not given by Eq. (4.4) but rather raised to the larger value 0.10. This adjustment yields the correct first moment, known from Appendix A to equal 0.52. Substituting from Eqs. (2.30) and (4.1) and integrating by parts expresses this moment condition in terms of the spectral function as

$$\left\langle \frac{1}{s} \right\rangle = \frac{\int \frac{ds}{d} f'}{\int ds f'} = \int_{s_0}^{\infty} \frac{ds}{s^2} f(s) . \tag{4.10}$$

The larger value of b required by Eq. (4.10) can be considered to take into account the higher order terms neglected in the truncation of the high-frequency expansion at three terms. We keep a, however, fixed by Eq. (4.3) which for $A = 1$ gives $a = 0.68$.

By interpolation between the dot-dash and solid curve we can generate a smooth monotonic curve for $f(s)$ which rises continuously from the true threshold at $s = \frac{1}{4}$ and has all of the required properties. The extra low-frequency tail adds, however, approximately 10% to the moment. Therefore the solid curve has been shifted to the right, corresponding to a larger value of b and s_0, as shown by the dashed curve in Fig. 1. The dotted, lowest portion of this curve has been replaced by the tail extending down to the true cutoff. The result is, we believe, a fairly accurate representation of $f(s)$ over the entire range $\frac{1}{4} \leq s < \infty$. Both the dashed curve (with the tail) and the solid curve (with no tail) satisfy Eq. (4.10) with $\langle s^{-1} \rangle = 0.52$. For the calculations in the next section we will use the solid curve, regarding it as a reasonable approximation to the dashed one, and much more convenient to work with. A further, much rougher approximation is shown by the solid curve labeled 2, which represents the two-term approximant

$$f(s) = 1 - \frac{1}{s} , \tag{4.11}$$

for $s \geq 1$. Equation (4.10) yields the rounded-off value $\langle s^{-1} \rangle = 0.50$. An even cruder approximation, which is nevertheless useful, as will be seen in the next section, is the step function (not shown in Fig. 1)

$$f(s) = \Theta(s - 2) . \tag{4.12}$$

The abrupt threshold at $s = 2$ is adjusted to give the same moment $\langle s^{-1} \rangle = 0.50$.

To demonstrate the effect of the various approximations described above, it is useful to study the relaxation rate along the positive imaginary frequency axis. We therefore introduce $z = -i\Omega$. In terms of this variable, Eq. (3.15) reads

$$\tilde{\Gamma} = \left\langle \ln\left(1 + \frac{z}{p^3 + A^{-1}p'^3}\right) \right\rangle . \tag{4.13}$$

Cauchy's theorem in its subtracted form applied to Eqs. (4.1) and (4.13) becomes

$$\tilde{\Gamma} = z \int_{s_0}^{\infty} \frac{ds}{s(s+z)} f(s) . \tag{4.14}$$

Equation (4.14) provides a linear frequency dependence in the low-frequency range $(0 \leq z \ll 1)$ with the slope given by the first moment

$$\left\langle \frac{1}{p^3 + A^{-1}p'^3} \right\rangle = \int_{s_0}^{\infty} \frac{ds}{s^2} f(s) , \tag{4.15}$$

in accord with Eqs. (2.29) and (2.30).

For the range $z \gg 1$ it is convenient to introduce

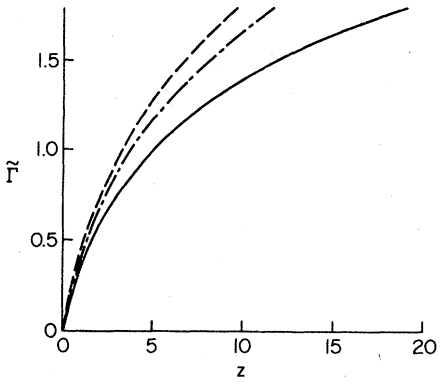

FIG. 2. Rate function versus frequency variable $z = -i\Omega$. The dashed, dot-dash and, solid curves are based on the one-, two-, and three-term approximants, respectively, all normalized to the same initial slope.

the complementary spectral function

$$\bar{f}(s) = 1 - f(s), \tag{4.16}$$

in terms of which Eq. (4.14) becomes

$$\begin{aligned}\tilde{\Gamma} &= z\int_{s_0}^{\infty}\frac{ds}{s(s+z)} - z\int_{s_0}^{\infty}\frac{ds}{s(s+z)}\bar{f}(s)\\ &= \ln\left(1+\frac{z}{s_0}\right) - z\int_{s_0}^{\infty}\frac{ds}{s(s+z)}\bar{f}(s)\\ &\simeq \ln\frac{z}{s_0} - \int_{s_0}^{\infty}\frac{ds}{s}\bar{f}(s)\\ &= \ln z + C\,.\end{aligned} \tag{4.17}$$

The approximations are permitted by $z \gg s_0$ and by the fact that the integral converges over a range where $s = O(1)$. The "spectral deficit" is

$$C = \langle \ln(p^3 + A^{-1}p'^3)\rangle = \ln s_0 + \int_{s_0}^{\infty}\frac{ds}{s}\bar{f}(s)\,, \tag{4.18}$$

and can also be written as $C = \ln s_1$, where s_1 is an effective step threshold. The value of C distinguishes between different spectral functions having the same first moment, but different shapes. Generally, a spectral function rising more more gradually from threshold will have a larger spectral deficit. This is readily illustrated by the comparison of the step function, for which $C = -\ln\langle s^{-1}\rangle$, with the two-term approximant of Eq. (4.11), for which $C = 1 - \ln 2 - \ln\langle s^{-1}\rangle$. The three-term approximant with the same value of $\langle s^{-1}\rangle$ has an even larger value of C.

The full course of $\tilde{\Gamma}$ vs z for the one-, two-, and three-term spectral functions is shown in Fig. 2 by the dashed, dot-dash, and solid curves, respectively. These are all calculated for $A = 1$ and therefore all have the same initial slope corresponding to the first moment $\langle s^{-1}\rangle = 0.52$. As explained in the preceding paragraph, in the range $z \gg 1$ the curves lie successively below one another because of their progressively increasing spectral deficits. From Fig. 2 it is clear that for low-frequency or long-time behavior a two-term or even one-term approximant may be adequate. On the other hand, for high-frequency or short-term behavior, such approximations may entail considerable error.

Let us now estimate the error incurred in neglecting the tail of the dashed curve in Fig. 1. This is the part of the spectral function which connects its high-frequency three-term approximant with the true threshold at $s = \frac{1}{4}$. The change in going from the solid curve to the dashed curve is, from Eqs. (4.14) and (4.17) for $z \gg 1$,

$$\begin{aligned}\Delta C &= -\int\frac{ds}{s}\Delta f\\ &= -\int\frac{f_T}{s}ds + \Delta b\int_{s_0}^{\infty}\frac{ds}{s^2}\\ &= -\int\frac{f_T}{s}ds + \frac{\Delta b}{s_0}\\ &\simeq s_0\left(-\int\frac{f_T}{s^2}ds + \frac{\Delta b}{s_0^2}\right),\end{aligned} \tag{4.19}$$

where f_T is the "tail" portion (i.e., the amount by which the dashed curve is above the dotted curve). The approximation in the last line of Eq. (4.19) is permitted by the fact that the tail is concentrated in the vicinity of $s = s_0$. Equation (4.19) can be compared with the change in the first moment

$$\begin{aligned}\Delta\left\langle\frac{1}{s}\right\rangle &= \int\frac{ds}{s^2}\Delta f\\ &= \int\frac{f_T}{s^2}ds - \Delta b\int_{s_0}^{\infty}\frac{ds}{s^3}\\ &= \int\frac{f_T}{s^2}ds - \frac{\Delta b}{2s_0^2}.\end{aligned} \tag{4.20}$$

But the dashed curve is adjusted so that there is no change in the moment, which requires

$$\frac{\Delta b}{s_0^2} = 2\int\frac{f_T}{s^2}ds = 2\Delta_T\left\langle\frac{1}{s}\right\rangle. \tag{4.21}$$

$\Delta_T\langle s^{-1}\rangle$ is the change produced by the tail alone, which as mentioned above, is 10% of $\langle s^{-1}\rangle$, or approximately equal to 0.05. Substitution of Eq. (4.21) into Eq. (4.19) yields

$$\Delta C \simeq s_0\Delta_T\left\langle\frac{1}{s}\right\rangle \simeq 0.025\,. \tag{4.22}$$

This result signifies that the true spectral function (dashed curve in Fig. 1) would yield a plot of $\tilde{\Gamma}$ vs z in Fig. 2 slightly below the solid curve. The amount of shift indicated by Eq. (4.22) is,

however, completely negligible, being an order of magnitude smaller than $1-\ln 2=0.31$, the difference of the spectral deficits of the two upper curves of Fig. 2. This serves to establish the accuracy of the three-term spectral function.

A further check on the three-term approximant comes from the actual numerical value of the spectral deficit. With

$$\bar{f}(s)=as^{-1/3}+bs^{-1}, \tag{4.23}$$

and the threshold value

$$\bar{f}(s_0)=as_0^{-1/3}+bs_0^{-1}=1, \tag{4.24}$$

we obtain

$$\int \frac{ds}{s}\bar{f}=3as_0^{-1/3}+bs_0^{-1}=3-2bs_0^{-1}. \tag{4.25}$$

Substituted into Eq. (4.18) this gives

$$C=\langle \ln(p^3+A^{-1}p'^3)\rangle=\ln s_0+3-2\frac{b}{s_0}. \tag{4.26}$$

To compare this result numerically with the Perl-Ferrell[16] value we have to take into account the fact that all of the above discussion has been based on $A=1$, while Eq. (3.10) gives the true value as $A=0.734$. As explained in Sec. III this results in a 10% reduction in the moment which happens to correspond to the difference between the dashed and solid curves in Fig. 1. Therefore we can use Eq. (4.21) to obtain the required increase in b as

$$\Delta b=2s_0^2\Delta_T\langle s^{-1}\rangle=0.03.$$

This raises b from 0.10 to 0.13. A more precise calculation gives $b=0.14$ and a new threshold at $s_0=0.65$, as shown in Fig. 1 by the dotted extension of the dashed curve. With these parameters Eq. (4.26) gives $C=2.14$, in good agreement with $3\times 0.60-\ln A=2.11$, the Perl-Ferrell value as expressed by Eq. (3.26). As the latter was obtained in a completely different way, this check is a convincing indication of the reliability of our three-term approximant. With this background, we proceed in the next section to use the three-term approximant for calculating the time-dependent deviation function.

We conclude this section with an additional criterion for distinguishing the different curves of Fig. 2. From Eq. (4.14) we obtain the moment expansion

$$\tilde{\Gamma}=\langle s^{-1}\rangle z-\tfrac{1}{2}\langle s^{-2}\rangle z^2+\cdots, \tag{4.27}$$

where

$$\langle s^{-n}\rangle=n\int_{s_0}^{\infty}\frac{ds}{s^{n+1}}f(s). \tag{4.28}$$

The second moment depends upon the shape of the spectral function. According to the type of approximant we find

$$\frac{\langle s^{-2}\rangle}{\langle s^{-1}\rangle^2}=\begin{cases}1, & \text{1 term} \quad (4.29a)\\ \frac{4}{3}, & \text{2 term} \quad (4.29b)\\ 2, & \text{3 term} \quad (4.29c)\end{cases}$$

substituting Eq. (4.29c) into Eq. (4.27) gives

$$\begin{aligned}\tilde{\Gamma}&=\langle s^{-1}\rangle z-(\langle s^{-1}\rangle z)^2+\cdots\\ &=\tfrac{1}{2}[2\langle s^{-1}\rangle z-\tfrac{1}{2}(2\langle s^{-1}\rangle z)^2+\cdots]\\ &\simeq\tfrac{1}{2}\ln(1+2\langle s^{-1}\rangle z),\end{aligned} \tag{4.30}$$

where the final line is suggested by the requirement of logarithmic asymptotic behavior. Equation (4.30) yields a good fit to the solid curve in Fig. 2 and is the approximation used by Ohta.[19] It corresponds to the single-step spectral function

$$f(s)=\tfrac{1}{2}\Theta(s-s_0), \tag{4.31}$$

where $s_0=2^{-1}\langle s^{-1}\rangle^{-1}\simeq 1$. The requirement $f(\infty)=1$ can be satisfied by the addition of a second step at $s=s_1$. If $s_1\gg s_0$ the first moment will be not be appreciably affected. The value of s_1 can be determined from the spectral deficit. According to Eq. (4.18) we have

$$C=\tfrac{1}{2}\ln(s_0s_1). \tag{4.32}$$

Setting this equal to the Perl-Ferrell value of $C=2.11$ and substituting $s_0=1$ from above gives $s_1=\exp 4.22=68.0$.

V. TIME-DEPENDENT CORRELATION FUNCTION

With the above results we are now in a position to calculate the time-dependent correlation function based upon the three-term spectral function

$$f(s)=1-0.68s^{-1/3}-0.14s^{-1} \tag{5.1}$$

for $s\geq s_0=0.65$. According to Eq. (2.17) the curvature function is

$$\tilde{B}(\tau)\equiv\frac{d^2}{d\tau^2}(e^{\tau}\Delta\tilde{G})=e^{\tau}\int_{s_0}^{\infty}ds\,f(s)e^{-\tau s}. \tag{5.2}$$

The substitution of Eq. (5.1) into Eq. (5.2) gives integrations which can be carried out by means of the integral exponential function

$$\mathrm{Ei}(x)=\mathrm{P}\int_{-\infty}^{x}\frac{dt}{t}e^{\tau} \tag{5.3}$$

and the incomplete Γ function,

$$\Gamma(n,y)=\int_y^{\infty}dt\,t^{n-1}e^{-t}. \tag{5.4}$$

Thus,

$$\tilde{B}(\tau)=e^{\tau}\frac{1}{\tau}e^{-s_0\tau}-0.68\tau^{-2/3}\Gamma(\tfrac{2}{3},s_0\tau)+0.14\,\mathrm{Ei}(-s_0\tau). \tag{5.5}$$

The two-term approximant of Eq. (4.11), with the threshold now at $s_0 = 1$, leads to the simpler expression

$$\tilde{B}(\tau) = \tau^{-1} + \mathrm{Ei}(-\tau), \tag{5.6}$$

The even cruder step function $f(s) = \Theta(s-2)$ gives

$$\tilde{B}(\tau) = \tau^{-1} e^{-\tau}. \tag{5.7a}$$

The weakened step function of Eq. (4.31) gives

$$\tilde{B}(\tau) = \frac{1}{2}\tau^{-1}. \tag{5.7b}$$

The first three of these functions are shown in Fig. 3 by the solid, the dot-dash, and the dashed curves, respectively. It will be noted that the cruder approximations overestimate the curvature, but that the error vanishes for $\tau \gtrsim 1$. It is interesting further to note that if we had only Eq. (5.6) and (5.7) and not the more complicated expression of Eq. (5.5), we could nevertheless get a rough estimate of the location of the solid curve by extrapolating down from the two other curves of Fig. 3.

The deviation function is calculated by substituting Eq. (5.1) into Eq. (4.1) and Eq. (2.19). We carry this out first for the simpler one- and two-term approximants. The step function gives

$$\begin{aligned} e^{\tau}\Delta\tilde{G} &= \int_2^{\infty} \frac{ds}{(s-1)^2}\left(e^{-(s-1)\tau} - 1\right) + \tau \ln 2 \\ &= \tau \int_{\tau}^{\infty} \frac{du}{u^2}\left(e^{-u} - 1\right) + \tau \ln 2 \\ &= \tau\left[\mathrm{Ei}(-\tau) + \ln 2\right] + e^{-\tau} - 1, \end{aligned} \tag{5.8a}$$

where the last line follows from an integral by parts and the substitution of Eq. (5.3). Equation (5.7b) leads to

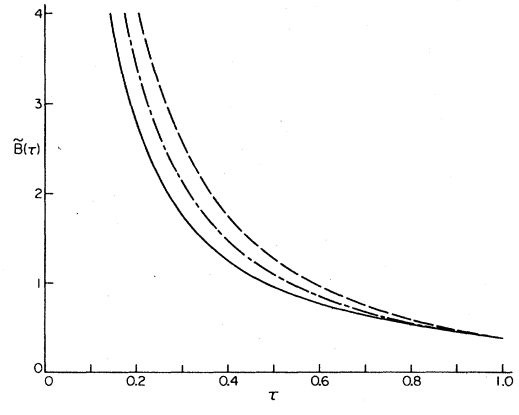

FIG. 3. Curvature function versus reduced time τ. The dashed, dot-dash, and solid curves are based upon the one-, two-, and three-term approximants, respectively.

$$e^{\tau}\Delta\tilde{G} = \tfrac{1}{2}\tau \ln\tau - \tfrac{1}{2}(1 - \ln\gamma), \tag{5.8b}$$

where $\ln\gamma = 0.5772$ is Euler's constant. Similarly for the two-term spectral function we find

$$e^{\tau}\Delta\tilde{G} = e^{\tau}\,\mathrm{Ei}(-\tau) + \tau - \ln\tau - \ln\gamma. \tag{5.9}$$

Unfortunately, it is not possible to carry out the necessary integration for the three-term spectral function in terms of known tabulated functions. Therefore, we have had to resort in Appendix D to a series expansion. In Fig. 4 one-, two-, and three-term results are exhibited by the dashed, dot-dash, and solid curves, respectively. Just as in Fig. 3, it is also apparent in Fig. 4 that the cruder approximants overestimate the effect. The more refined three-term spectral function gives a curve for the deviation function which lies above the other two curves. It is this curve which is the most reliable one according to the discussion in Sec. IV and which we compare in Fig. 5 with the experimental data of Burstyn, Chang, and Sengers.[6] This data has been gathered into bins of width $\Delta\tau = 0.1$. The arrow bars show the the standard deviations for each bin. Because of the factor e^{τ} the standard deviation is larger for the bins corresponding to larger values of τ. It is evident that the theoretical curve gives a good representation of the experimental data. It is worth emphasizing that this agreement has been accomplished *without* any fitting parameter whatsoever. The two parameters of the theory, z_η and A, have been fixed by information from other sources, totally independent of the experiment of Burstyn *et al.*[6]

VI. TEMPERATURE DEPENDENCE

The temperature dependence of the effect studied in the preceding section is readily visualized in terms of the three-term spectral function of Eq.

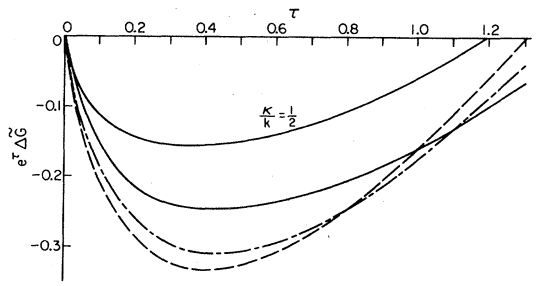

FIG. 4. e^{τ} times the deviation function versus reduced time τ. The dashed, dot-dash, and solid curves correspond to the one-, two-, and three-term approximants, respectively. The solid curve labeled $\kappa/k = \frac{1}{2}$ is based upon the three-term approximant at an elevated temperature.

(4.2). Both coefficients a and b increase with rising temperature, as shown in detail in Appendix E (as a function of κ, the reciprocal of the correlation length). As a consequence, the threshold of the spectral function recedes toward higher frequencies, with the asymptotic limit staying constant, however, at $f(\infty)=1$. The spectral function for $\kappa/k=\frac{1}{2}$ is shown by the right-hand solid curve in Fig. 1. The threshold has receded from $s_0=0.65$ out to $s_0=1.28$. This can be understood qualitatively from the fact that as κ increases the characteristic frequency for the viscosity varies as κ^3. The reference relaxation rate for wave number k varies, however, as κk^2. The threshold frequency variable s_0 can be expected therefore to vary as a linear function of κ^2/k^2, which in turn implies for the first moment

$$\langle s^{-1}\rangle^{-1}=2(1+b_1\kappa^2/k^2)\,, \tag{6.1}$$

where we have rounded off the $\kappa=0$ value of $\langle s^{-1}\rangle$ to 0.50. The value of b_1 follows from Appendix E, or alternatively and more directly from the detailed study of $\langle s^{-1}\rangle$ in Appendix A. The two determinations are consistent for $A=1$ and yield $b_1=4.8$, which substituted into Eq. (6.1) gives $\langle s^{-1}\rangle=0.24$ for $\kappa/k=\frac{1}{2}$.

Proceeding now just as we did for $\kappa=0$, we obtain for $\kappa/k=\frac{1}{2}$ the uppermost curve in Fig. 4 from the series expansion of Appendix D. This curve is replotted in Fig. 6 along with the data of Burstyn, Chang, and Sengers[6] for the nearby value of $\kappa/k=0.42$ (corresponding to $T-T_c=11.7$ mK). It can be seen by comparing the curves in Figs. 5 and 6 that the theory predicts a decrease of approximately 38% in the maximum deviation as a result of the rise in temperature. It is evident that the data are in very good accord with this prediction.

Although the above type of computation can be carried out for any temperature, it would be useful to have a simple measure for the temperature

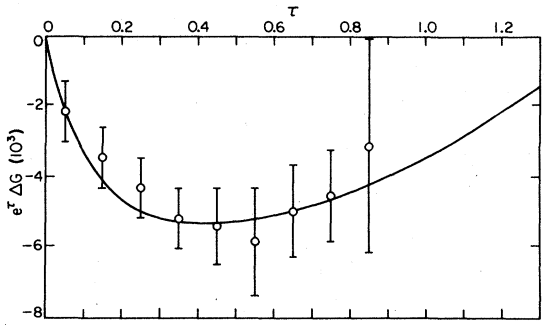

FIG. 5. e^{τ} times the deviation function versus reduced time τ. The experimental data are from Ref. 6.

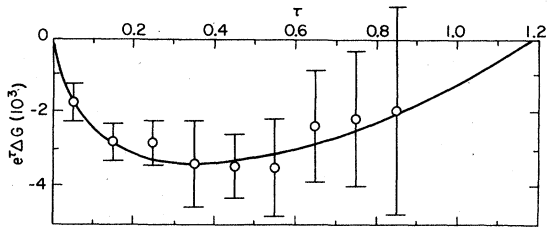

FIG. 6. e^{τ} times the deviation function versus reduced time τ at the elevated temperature such that the correlation length is π^{-1} times the wavelength of the fluctuation. The experimental data are from Ref. 6.

dependence of the deviation. Burstyn *et al.*[6] adopted for this purpose the curvature of the best-fit parabola. We have found, however, that this approach can be misleading, as it tends to de-emphasize the "hook", or steep left-hand portion of the curve for $e^{\tau}\Delta G$. Therefore, we prefer to characterize the curvature by the integral of the deviation function over the interval $0\leq\tau\leq\tau_1$, where τ_1 is the (first) zero of $\Delta\tilde{G}$. The mean value of the curvature function $\tilde{B}$ [Eq. (5.2)] is related to the integral by

$$\int_0^{\tau_1}\Delta\tilde{G}\,d\tau=-\tfrac{1}{12}\tau_1^3\langle\tilde{\tilde{B}}\rangle\,, \tag{6.2}$$

the "double tilde" indicating the simplification of dropping the factor e^{τ}.

Because the zero of $\Delta\tilde{G}$ plays an important role in our work it is useful to exhibit the full course of this function. This is shown for $\kappa=0$ in Fig. 7, with the zero occurring at $\tau_1=1.37$. Although Fig. 7 is based on Eq. (5.10) and the simpler two-term approximant, it serves to illustrate the general features of $\Delta\tilde{G}$. (The more accurate three-term spectral function, according to the series expansion of Appendix D, gives $\tau_1=1.49$.) It is evident that the area under the curve for $\tau\geq\tau_1$ is sufficient to balance the integration for $0\leq\tau\leq\tau_1$, so as to satisfy the zero-frequency sum rule of Eq.

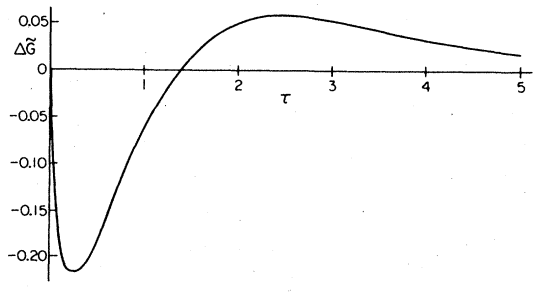

FIG. 7. Deviation function versus reduced time τ for the two-term approximant, exhibiting the zero at $\tau_1=1.37$.

(2.10). This sum rule enables us to relate the integration required in Eq. (6.2) to the rest of the function according to

$$\int_0^{\tau_1} \Delta\tilde{G}\, d\tau = -\int_{\tau_1}^{\infty} \Delta\tilde{G}\, d\tau = -\frac{1}{\langle\tau\rangle}\int_{\tau_1}^{\infty} \Delta G\tau\, d\tau$$
$$\simeq -\frac{1}{\langle\tau\rangle}\int_0^{\infty} \Delta\tilde{G}\tau\, d\tau = -\langle\tau\rangle^{-1}\langle s^{-1}\rangle . \quad (6.3)$$

Here, after introducing an average τ, defined for $\tau \geq \tau_1$, we have approximated the integral by the actual first moment of τ. This is justified on the basis that the contribution from $0 \leq \tau \leq \tau_1$ to the moment is small compared to the contribution from $\tau \geq \tau_1$. The final form of Eq. (6.3) follows from substitution of Eq. (2.33). Identifying Eq. (6.3) with Eq. (6.2), we obtain the temperature dependence

$$\langle\tilde{\tilde{B}}\rangle \propto \tau_1^{-4}\langle s^{-1}\rangle . \quad (6.4)$$

(Here we have introduced the further assumption $\langle\tau\rangle \propto \tau_1$, dictated by the idea that τ_1 sets the overall time scale.)

Because of the rather rough approximations made in deriving (6.4), it is desirable to confirm it by an alternative derivation. This is obtained by considering the Laplace transform

$$\Delta\tilde{g} = \int_0^{\infty} d\tau\, e^{-z\tau}\Delta\tilde{G}(\tau) . \quad (6.5)$$

According to Eq. (2.31), the integral is equal to

$$\Delta\tilde{g} = -\frac{\tilde{\Gamma}}{(1-z)^2} , \quad (6.6)$$

and has the initial slope

$$\left.\frac{d\Delta\tilde{g}}{dz}\right|_{z=0} = -\left.\frac{d\tilde{\Gamma}}{dz}\right|_{z=0} = -\left\langle\frac{1}{s}\right\rangle . \quad (6.7)$$

Equation (6.6) is plotted as the solid curve in Fig. 8 and it will be noted that the function exhibits a minimum at $z \simeq \tau_1^{-1}$. This is because the integral of Eq. (6.2) is approximately simulated by Eq. (6.5). With $z \simeq \tau_1^{-1}$ the region $0 \leq \tau \leq \tau_1$ contributes negatively while at the same time, because of the exponential factor, the positive contribution from $\tau \geq \tau_1$ is suppressed. Combining these considerations with the initial slope of Eq. (6.7), we obtain

$$(\Delta\tilde{g})_{\min} \propto -\tau_1^{-1}\langle s^{-1}\rangle . \quad (6.8)$$

Identifying Eqs. (6.8) and (6.2) leads again to Eq. (6.4).

In order to make use of Eq. (6.4) we need to establish the temperature dependence of the separate factors τ_1^{-4} and $\langle s^{-1}\rangle$. The latter is specified by Eq. (6.1). The required information on the temperature dependence of τ_1 is obtained from the

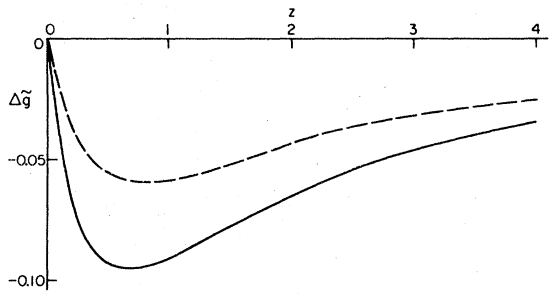

FIG. 8. Laplace transform of the deviation function versus frequency variable $z = -i\Omega$. The shift of the minimum to the right at the elevated temperature (dashed curve) reflects the decrease in τ_1.

two-term truncation of Eq. (4.30),

$$\tilde{\Gamma} \simeq \langle s^{-1}\rangle z - (\langle s^{-1}\rangle z)^2 . \quad (6.9)$$

Substituting Eq. (6.9) into Eq. (6.6), we find to second order in z

$$\Delta\tilde{g} \simeq -z\langle s^{-1}\rangle[1 - (2 + \langle s^{-1}\rangle)z] . \quad (6.10)$$

Equation (6.10) mimics the true z dependence of $\Delta\tilde{g}$ shown in Fig. 8, in that the linear behavior for $0 \leq z \ll 1$ is modified by the second term so as to produce a minimum at

$$z_1 = (1 + \tfrac{1}{2}\langle s^{-1}\rangle)^{-1} . \quad (6.11)$$

Identifying z_1 with τ_1^{-1} and raising it to the fourth power gives the desired approximate proportionality

$$\tau_1^{-4} \propto (1 + 2\langle s^{-1}\rangle)^{-1} . \quad (6.12)$$

Equation (6.12) has the considerable advantage that it reduces the entire problem of the temperature dependence to the variation of a single parameter, the moment $\langle s^{-1}\rangle$. The dashed curve in Fig. 8 exhibits the shift in τ_1^{-1} described by Eq. (6.11). It is drawn for $\langle s^{-1}\rangle = 0.24$, one-half of the $\kappa = 0$ value. Because the minimum is shifted in the direction of increasing z the value of $(\Delta\tilde{g})_{\min}$ is not decreased by the full factor of one-half. This illustrates how the shift of τ_1^{-1} tends to counteract the temperature dependence of $\langle s^{-1}\rangle$.

Substitution of Eqs. (6.12) and (6.1) into Eq. (6.4) gives for the temperature dependence of the curvature

$$\tilde{\tilde{B}} \propto \tau_1^{-4}\langle s^{-1}\rangle \propto \frac{\langle s^{-1}\rangle}{1 + 2\langle s^{-1}\rangle}$$
$$= \frac{1}{\langle s^{-1}\rangle^{-1} + 2} = \frac{1/2}{2 + b_1(\kappa^2/k^2)} . \quad (6.13)$$

It is convenient to normalize the curvature to its $\kappa = 0$ value, $\tilde{\tilde{B}}_0$, by the ratio $K_2 = \tilde{\tilde{B}}/\tilde{\tilde{B}}_0$. Thus we obtain

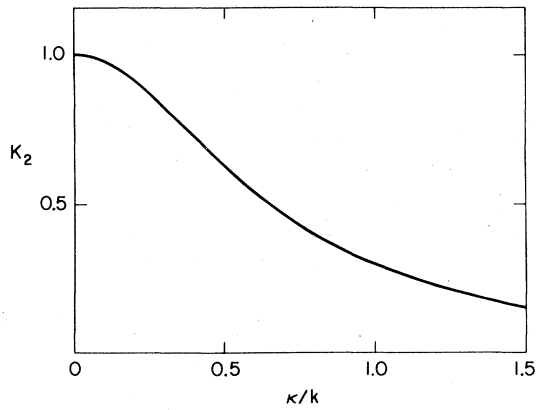

FIG. 9. Curvature versus κ/k. κ^{-1} is the temperature-dependent correlation length and k is the scattering wave number.

$$K_2=\frac{1}{1+b_2(\kappa^2/k^2)}, \tag{6.14}$$

with $b_2=b_1/2=2.4$. Equation (6.14) is plotted in Fig. 9 and provides the desired continuous description of the temperature dependence of the curvature. Substituting $\kappa/k=\frac{1}{2}$ into Eq. (6.14) gives $K_2=\frac{5}{8}=0.625$, which can be compared with the 38% decrease found from comparison of Fig. 6 with Fig. 5. [This close agreement is somewhat fortuitous because the factor $\exp\tau$ is lacking from the work leading to Eq. (6.14). Furthermore, a factor of τ_1^2 should be taken into account when comparing the maximum deviation with the curvature.]

VII. SUMMARY

We have shown how the frequency dependence of the viscosity leads to a significant frequency dependence of the diffusion coefficient. This shows up as a deviation from pure exponential decay for the time-dependent correlation function of the concentration fluctuations. Our calculated deviation compares well with the measurements of Burstyn, Chang, and Sengers[6] at the critical point, where the correlation length is infinite. As the temperature is raised, the correlation length becomes finite and the effect decreases as well. Our computed temperature dependence for the curvature of the semi-log plot of the correlation function agrees well with the observed temperature dependence. As in the case of $T=T_c$, the agreement for $T>T_c$ results without the introduction of any fitting parameter. It is also worth noting that the frequency dependence of the viscosity,[20] which forms the backbone of the calculation, may have been detected in recent measurements on carbon dioxide near the critical point.

We conclude by remarking that the above calculation makes the classical fluid share the common characteristic of nonexponential decay of fluctuations, which has been already calculated for liquid helium, antiferromagnets, and isotropic ferromagnets. The deviation from the exponential shape is a crucial point in critical dynamics, showing the existence of non-Markoffian effects. This should serve as a warning to recent attempts to fashion a theory for critical dynamics by ignoring the non-Markoffian effects at every stage of iteration of a real space renormalization group.

ACKNOWLEDGMENTS

We acknowledge support from the National Science Foundation under Grants PHY77-27084 from the Institute for Theoretical Physics, University of California, Santa Barbara, and DMR79-01172, 79-00908, and 79-10819 from the University of Maryland. We are also indebted to Dr. H. Burstyn, Dr. R. F. Chang, and Dr. J. V. Sengers for numerous stimulating discussions.

APPENDIX A: THE FIRST MOMENT

In this appendix we calculate the first moment at $T=T_c$, and the first change that sets in when the temperature is raised above T_c. To permit analytic evaluation, A will be set equal to 1 in this section. The κ-dependent generalization of Eqs. (3.15), correct to $O(\kappa^2)$, κ being the inverse correlation length, is

$$\tilde{\Gamma}(\Omega)=\left\langle\ln\left(1-\frac{-i\Omega}{p^3+p'^3[1+\eta_1(\kappa^2/p'^2)]}\right)\right\rangle, \tag{A1}$$

where all momenta are scaled to set the external momentum equal to 1. κ is also measured in units of k. Note that p^3 has not acquired any κ^2 correction, because the Kawasaki function does not have a term of $O(\kappa^2)$. The scale for the frequency dependence of the viscosity, however, changes with temperature as $O(\kappa^2)$ and hence p'^3 is altered by the factor $[1+\eta_1(\kappa^2/p'^2)]$. The coefficient η_1 will be determined later in this appendix. At a finite correlation length $\xi=\kappa^{-1}$, Eqs. (3.16)–(3.18) generalize to

$$\langle L\rangle=\frac{1}{4\pi\bar{I}}\int\frac{d^3p'}{p^2+\kappa^2}\frac{\sin^2\theta'}{p'^2}L, \tag{A2}$$

$$\bar{I}=\frac{1}{4\pi}\int\frac{d^3p'}{p^2+\kappa^2}\frac{\sin^2\theta'}{p'^2}=\frac{\pi}{3}K(\kappa)\frac{\kappa}{1+\kappa^2}$$

$$\simeq\frac{\pi^2}{8}\frac{1}{1+\kappa^2}+O(\kappa^4), \tag{A3}$$

and

$$i\tilde{\Gamma}'(0)=\left\langle \frac{1}{p^3+p'^3[1+\eta_1(\kappa^2/p'^2)]}\right\rangle=\left\langle\frac{1}{s}\right\rangle . \quad \text{(A4)}$$

[$K(\kappa)$ is the Kawasaki function.]

We first study the $\kappa=0$ behavior. In this case $I=\pi^2/8$ and we have

$$\frac{\pi^2}{8}\left\langle\frac{1}{s}\right\rangle=\frac{1}{4\pi}\int\frac{d^3p'}{p^2p'^2}\frac{\sin^2\theta'}{p^3+p'^3}. \quad \text{(A5)}$$

The convenient way of evaluating such integrals is the introduction of the bipolar coordinates. We write

$$p^2=p'^2+1-2p'\cos\theta', \quad \text{(A6)}$$

and we use it to eliminate the angle variable by

$$p'\sin\theta'\,d\theta'=p\,dp \quad \text{(A7)}$$

and

$$\sin^2\theta'=1-\frac{(1-p^2+p'^2)^2}{4p'^2}. \quad \text{(A8)}$$

The further substitution of

$$x=p+p' \quad \text{(A9a)}$$

and

$$y=p-p' \quad \text{(A9b)}$$

puts Eqs. (A8) and (A5) into the form

$$\sin^2\theta'=\frac{(x^2-1)(1-y^2)}{(x-y)^2} \quad \text{(A10)}$$

and

$$\frac{\pi^2}{8}\left\langle\frac{1}{s}\right\rangle=\int_1^\infty\frac{dx}{x}\int_{-1}^1 dy\,\frac{(x^2-1)(1-y^2)}{(x^2-y^2)(x-y)^2}\frac{4}{x^2+3y^2}$$

$$=8\int_1^\infty\frac{x^2-1}{x}\int_0^1 dy\,\frac{(1-y^2)(x+y)^2}{(x^2-y^2)^3(x^2+3y^2)}. \quad \text{(A11)}$$

The resulting integrals can now be evaluated by elementary techniques to yield

$$\frac{\pi^2}{8}\left\langle\frac{1}{s}\right\rangle=\frac{4\pi}{15}+\frac{8\ln 2}{15}-\frac{29}{140}-\frac{8\sqrt{3}\ln 2}{45}-\frac{117\sqrt{3}}{1440}$$

$$\simeq 0.646, \quad \text{(A12)}$$

giving

$$\left\langle\frac{1}{s}\right\rangle=0.52. \quad \text{(A13)}$$

We turn now to the temperature dependence. The first effect of a finite correlation length is found by linearizing Eq. (A5) in κ^2 to get

$$\frac{\pi^2/8}{1+\kappa^2}\left\langle\frac{1}{s}\right\rangle=\frac{1}{4\pi}\int\frac{d^3p}{p^2p'^2}\frac{\sin^2\theta'}{p^3+p'^3}$$

$$-\kappa^2\left(\frac{1}{4\pi}\int\frac{d^3p}{p^4p'^2}\frac{\sin^2\theta'}{p'^3+p^3}\right.$$

$$\left.+\frac{\eta_1}{4\pi}\int\frac{d^3p}{p^2p'^2}\frac{\sin^2\theta'p'}{(p^3+p'^3)^2}\right)+\cdots. \quad \text{(A14)}$$

Now,

$$\frac{1}{4\pi}\int\frac{d^3p}{p^2p'^2}\frac{p'\sin^2\theta'}{(p^3+p'^3)^2}=\frac{18\pi}{105\sqrt{3}}-\frac{32\ln 2}{315}+\frac{43}{420}$$

$$\simeq 0.343, \quad \text{(A15)}$$

and

$$\frac{1}{4\pi}\int\frac{d^3p}{p^2p'^2}\frac{\sin^2\theta'}{p^2(p^3+p'^3)}=\frac{99\ln 2}{105}-\frac{1353}{2520}+\frac{16\sqrt{3}\pi}{105}.$$

$$\simeq 0.946 \quad \text{(A16)}$$

Thus,

$$\frac{\pi^2}{8(1+\kappa^2)}\left\langle\frac{1}{s}\right\rangle\simeq 0.646-\kappa^2(0.343\,\eta_1+0.946)+\cdots. \quad \text{(A17)}$$

To determine η_1, we need the frequency derivative of the nonlocal viscosity η. The first variation of this derivative with κ^2 at zero frequency is

$$-\left.\frac{\partial\eta(k,\kappa,\omega)}{\partial(-i\omega)}\right|_{\omega=0}\propto\frac{1}{4\pi}\int\frac{d^3p}{p^2p'^2}\frac{p^2(p^2-p'^2)^2\sin^2\theta}{(p^3+p'^3)^2}$$

$$-\frac{\kappa^2}{2\pi}\int\frac{d^3p}{p^2p'^2}\frac{\sin^2\theta(p^2-p'^2)^2}{(p^3+p'^3)^2}$$

$$+O(\kappa^4). \quad \text{(A18)}$$

We find

$$\frac{1}{4\pi}\int\frac{d^3p}{p'^2}\frac{(p^2-p'^2)^2\sin^2\theta}{(p^3+p'^3)^2}$$

$$=\frac{1}{3}+\frac{\pi^2}{8}-\frac{1}{3\sqrt{3}}(2\pi+G+J)\simeq 0.0844, \quad \text{(A19)}$$

where G (Catalan's constant) $=0.916$ and

$$J=\int_1^{\sqrt{3}}(dx/x)\tan^{-1}x=0.505.$$

Equation (A19) agrees with the result of Perl and Ferrell,[16] whose notation we are using here.

$$\frac{1}{4\pi}\int\frac{d^3p}{p^2p'^2}\frac{\sin^2\theta(p^2-p'^2)^2}{(p^3+p'^3)^2}=\frac{17}{3}-\frac{9\pi^2}{16}+\frac{3\pi^2}{2}-\frac{221}{15}+\frac{27}{8}\left(\frac{158}{63}-\frac{2}{75}-\frac{\pi^2}{4}\right)$$

$$+\frac{1}{2}\left[\left(2G+2J-\frac{4\pi}{9}\right)\frac{1}{\sqrt{3}}-\frac{11}{15}\right]+\frac{3}{8}\left[\frac{28}{15}+\frac{12}{175}-\frac{1}{\sqrt{3}}\left(2G+2J+\frac{4\pi}{9}\right)+\frac{2}{3}\right]$$

$$\simeq 0.342\,. \tag{A20}$$

Consequently,

$$-\frac{\partial\eta(k,\kappa,\omega)}{\partial(-i\omega)}\bigg|_{\omega=0}\propto 1-8.10\kappa^2+\cdots\,, \tag{A21}$$

yielding

$$\eta_1=8.10\,. \tag{A22}$$

With the substitution of Eq. (A22), Eq. (A17) gives, to $O(\kappa^2)$,

$$\frac{\pi^2}{8}\left\langle\frac{1}{s}\right\rangle=0.646(1-4.76\,\kappa^2+\cdots)\,, \tag{A23}$$

the desired initial temperature dependence of the first moment.

APPENDIX B: HIGH-FREQUENCY SPECTRAL FUNCTION

In this appendix we present an alternative derivation of the three-term spectral function of Eq. (4.2). For simplicity we set $A=1$, for which Eq. (4.8) becomes

$$f'(s)=\langle\delta(p^3+p'^3-s)\rangle\,. \tag{B1}$$

For a fixed value of $\mu'=\cos\theta'$ we can eliminate p in terms of p' by means of

$$p^2=p'^2+2p'\mu'+1\,. \tag{B2}$$

The Dirac delta function of Eq. (B1) then imposes the approximate constraint

$$s\simeq 2p'^3+3p'^2\mu'+\tfrac{3}{2}p'(1+\mu'^2) \tag{B3}$$

from which we obtain

$$\frac{ds}{dp'}\simeq 6p'^2+6p'\mu'+\tfrac{3}{2}(1+\mu'^2)\,. \tag{B4}$$

The integration over the delta function brings in the reciprocal of Eq. (B4) so that to three-term accuracy the integrand for the remaining angle averaging becomes

$$p'^2\left(\frac{ds}{dp'}\right)^{-1}\simeq\frac{1}{6p'^4}-\frac{\mu'}{2p'^5}+\frac{1}{p'^6}\left(\frac{-5}{24}+\frac{27}{24}\mu'^2\right)\,. \tag{B5}$$

It remains to eliminate p' in terms of s. For this purpose we introduce

$$p_s\equiv\left(\frac{s}{2}\right)^{1/3}, \tag{B6}$$

and obtain from Eq. (B3) the required connection in descending powers of p_s as

$$p'\simeq p_s-\frac{\mu'}{2}-\frac{1}{4p_s}\,. \tag{B7}$$

Substituting Eq. (B7) into Eq. (B5) and carrying our the angle averaging (weighted according to $\sin^2\theta'=1-\mu'^2$) yields

$$\left\langle p^{-2}\left(\frac{ds}{dp'}\right)^{-1}\right\rangle_\Omega\simeq\frac{1}{6p_s^4}-\frac{\langle\mu'\rangle}{6p_s^5}+\frac{1}{p_s^6}\left(\frac{-1}{24}+\frac{7}{24}\langle\mu'^2\rangle_\Omega\right)$$

$$=\frac{1}{6p_s^4}+\frac{1}{60p_s^6}$$

$$=\frac{(2)^{1/3}}{3}s^{-4/3}+\frac{1}{15}s^{-2}\,, \tag{B8}$$

by virtue of Eq. (B6). The average occurring in Eq. (B1) is connected to the above angle averaging by the factor

$$I^{-1}\int_0^1 d\mu'(1-\mu'^2)=\frac{2}{3I}\,. \tag{B9}$$

Upon substitution of Eqs. (B8) and (3.17), Eq. (B1) therefore becomes

$$f'(s)=\frac{2}{3I}\left\langle p^{-2}\left(\frac{ds}{dp'}\right)^{-1}\right\rangle_\Omega$$

$$=\frac{16(2)^{1/3}}{9\pi^2}s^{-4/3}+\frac{16}{45\pi^2}s^{-2}\,. \tag{B10}$$

Integrating and imposing the boundary condition $f(\infty)=1$ gives consequently

$$f(s)=1-\frac{16(2)^{1/3}}{3\pi^2}s^{-1/3}-\frac{16}{45\pi^2}s^{-1}\,, \tag{B11}$$

in agreement with Eqs. (4.2), (4.3), and (4.4).

APPENDIX C: THRESHOLD SPECTRAL FUNCTION

According to Eqs. (4.7) and (3.17) the spectral function with A set equal to one is

$$f(s)=\langle\Theta(s-p^3-p'^3)\rangle$$

$$=\frac{2}{\pi^3}\int\frac{d^3p}{p^2p'^2}\sin^2\theta'\Theta(s-p^3-p'^3)\,. \tag{C1}$$

To find the threshold behavior we introduce the variable $p_{\vec{1}}$ in terms of which

$$\vec{p} = \tfrac{1}{2}\vec{1} + \tfrac{1}{2}\vec{p}_1 \tag{C2a}$$

and

$$\vec{p}' = \tfrac{1}{2}\vec{1} - \tfrac{1}{2}\vec{p}_1 , \tag{C2b}$$

where $\vec{1} = \vec{k}/k$, and work in the range $p_1 \ll 1$. If α is the angle between $p_{\vec{1}}$ and $\vec{1}$

$$\sin^2\theta' = 1 - \frac{(1+p_1\cos\alpha)^2}{(\vec{1}+\vec{p}_1)^2}$$

$$= \frac{p_1^2\sin^2\alpha - 2p_1\cos\alpha}{(\vec{1}+\vec{p}_1)^2} . \tag{C3}$$

In terms of the variable $\vec{p}_1$, Eq. (6.1) becomes

$$f(s) = \frac{4}{\pi^3}\int \frac{d^3p_1}{(\vec{1}+\vec{p}_1)^2(\vec{1}-\vec{p}_1)^2}\,\frac{p_1^2\sin^2\alpha - 2p_1\cos\alpha}{(1+\vec{p}_1)^2}$$

$$\times\Theta\left(s - \tfrac{1}{8}[(\vec{1}+\vec{p}_1)^3 + (\vec{1}-\vec{p}_1)^3]\right). \tag{C4}$$

Noting that

$$(\vec{1}+p_1)^3 + (\vec{1}-\vec{p}_1)^3 = 2 + 3p_1^2(1+\cos^2\alpha) + O(p_1^4), \tag{C5}$$

and consequently

$$\Theta\left(s - \tfrac{1}{8}[(1+\vec{p}_1)^3 + (1-\vec{p}_1)^3]\right)$$

$$\simeq \Theta\left(\Delta s - \tfrac{3}{8}p_1^2(1+\cos^2\alpha)\right), \tag{C6}$$

where $\Delta s = s - \frac{1}{4}$, we find

$$f(s) = \frac{8}{\pi^2}\int_0^{\pi}\sin^3\alpha\,d\alpha\int_0^{[8\Delta s/3(1+\cos^2\alpha)]^{1/2}} p_1^4\,dp_1$$

$$= \frac{8}{5\pi^2}\int_0^{\pi}\sin^3\alpha\,d\alpha\left(\frac{8}{3}\frac{\Delta s}{1+\cos^2\alpha}\right)^{5/2}$$

$$= \frac{1024}{45\pi^2}\frac{\sqrt{2}}{\sqrt{3}}\int_0^{\pi}\frac{\sin^2\alpha\,d\alpha}{(1+\cos^2\alpha)^{5/2}}(\Delta s)^{5/2}$$

$$= \frac{4096}{135\sqrt{3}\,\pi^2}(\Delta s)^{5/2}$$

$$\simeq 1.775(\Delta s)^{5/2} . \tag{C7}$$

This is the required threshold behavior of the spectral function and is shown as the dot-dash curve in Fig. 1.

APPENDIX D: CORRELATION FUNCTION

In this appendix, we present the results for $e^{\tau}G(\tau)$, when the full three-term spectral function

$$f(s) = 1 - a/s^{1/3} - b/s$$

is used in Eq. (4.2). The integration over s can be performed in closed form for the first and third terms of $f(s)$. Unfortunately, this is not true for the second term and we have to resort to a series expansion. The most convenient way of handling this is to consider the contributions of this term to the second derivative:

$$\frac{d^2}{d\tau^2}P\int_{s_0}^{\infty}\frac{ds}{s^{1/3}}\frac{e^{-(s-1)\tau}-1}{(s-1)^2} = e^{\tau}\int_{s_0}^{\infty}ds\,\frac{e^{-s\tau}}{s^{1/3}}$$

$$= \frac{e^{\tau}}{\tau^{2/3}}\Gamma(\tfrac{2}{3}) - e^{\tau}\int_0^{s_0}s^{-1/3}e^{-s\tau}ds$$

$$= \Gamma(\tfrac{2}{3})\sum_{n=0}^{\infty}\frac{\tau^{n-2/3}}{n!} - s_0^{2/3}e^{\tau}\sum_{n=0}^{\infty}\frac{(\tau s_0)^n(-1)^n}{n!\,(n+\frac{2}{3})}$$

$$= \Gamma(\tfrac{2}{3})\tau^{-2/3}\left(1+\tau+\frac{\tau^2}{2}+\frac{\tau^3}{6}+\frac{\tau^4}{24}+\cdots\right)$$

$$- s_0^{2/3}\left[\tfrac{3}{2} + (\tfrac{3}{2} - \tfrac{3}{5}s_0)\tau + (\tfrac{3}{4} - \tfrac{3}{5}s_0 + \tfrac{3}{16}s_0^2)\tau^2\right.$$

$$\left. + (\tfrac{1}{4} - \tfrac{3}{10}s_0 + \tfrac{3}{16}s_0^2 - \tfrac{1}{22}s_0^3)\tau^3 + (\tfrac{1}{16} - \tfrac{1}{10}s_0 + \tfrac{3}{32}s_0^2 - \tfrac{1}{22}s_0^3 + \tfrac{1}{112}s_0^4)\tau^4 + \cdots\right] . \tag{D1}$$

Integrating twice,

$$P\int_{s_0}^{\infty}\frac{ds}{s^{1/3}}\frac{e^{-(s-1)\tau}-1}{(s-1)^2} = \Gamma(\tfrac{2}{3})\tau^{4/3}(\tfrac{9}{4} + \tfrac{9}{28}\tau + \tfrac{9}{140}\tau^2 + \tfrac{3}{260}\tau^3 + \tfrac{3}{1664}\tau^4 + \cdots)$$

$$- s_0^{2/3}\left[\tfrac{3}{4}\tau^2 + (\tfrac{3}{2} - \tfrac{3}{5}s_0)\frac{\tau^3}{6} + (\tfrac{3}{4} - \tfrac{3}{5}s_0 + \tfrac{3}{16}s_0^2)\frac{\tau^4}{12} + (\tfrac{1}{4} - \tfrac{3}{10}s_0 + \tfrac{3}{16}s_0^2 - \tfrac{1}{22}s_0^3)\frac{\tau^5}{20}\right.$$

$$\left. + (\tfrac{1}{16} - \tfrac{1}{10}s_0 + \tfrac{3}{32}s_0^2 - \tfrac{1}{22}s_0^3 + \tfrac{1}{112}s_0^4)\frac{\tau^6}{30} + \cdots\right] + C\tau , \tag{D2}$$

where

$$C = \mathrm{P}\int_{s_0}^{\infty} \frac{ds}{s^{1/3}(s-1)} = \frac{\pi}{\sqrt{3}} + \int_0^{s_0} \frac{ds}{s^{1/3}(s-1)}$$

$$= \frac{\pi}{\sqrt{3}} + \ln \frac{(1+s_0^{1/3}+s_0^{2/3})^{1/2}}{1-s_0^{1/3}} - \sqrt{3}\left(\tan^{-1}\frac{1+2s_0^{1/3}}{\sqrt{3}} - \frac{\pi}{6}\right). \tag{D3}$$

The integrals

$$\mathrm{P}\int_{s_0}^{\infty} [ds/(s-1)^2](e^{-(s-1)\tau}-1)$$

and

$$\mathrm{P}\int_{s_0}^{\infty} (ds/s)[e^{-(s-1)\tau}-1)/(s-1)^2]$$

have already been evaluated in Sec. V. We are thus led to

$$\mathrm{P}\int_{s_0}^{\infty} ds f(s)\frac{e^{-(s-1)\tau}-1}{(s-1)^2} = [(1-b)\tau - b]\,\mathrm{Ei}((1-s_0)\tau) - (1-b)\frac{e^{(1-s_0)\tau}-1}{1-s_0} + b\ln\frac{1-s_0}{s_0} + be^{\tau}\mathrm{Ei}(-s_0\tau)$$

$$-a\Gamma(\tfrac{2}{3})\tau^{4/3}(\tfrac{9}{4} + \tfrac{9}{28}\tau + \tfrac{9}{140}\tau^2 + \tfrac{3}{260}\tau^3 + \tfrac{3}{1664}\tau^4 + \cdots)$$

$$+as_0^{2/3}[\tfrac{3}{4}\tau^2 + (\tfrac{3}{2} - \tfrac{3}{5}s_0)\frac{\tau^3}{6} + (\tfrac{3}{4} - \tfrac{3}{5}s_0 + \tfrac{3}{16}s_0^2)\frac{\tau^4}{12}$$

$$+(\tfrac{1}{4} - \tfrac{3}{10}s_0 + \tfrac{3}{16}s_0^2 - \tfrac{1}{22}s_0^3)\frac{\tau^5}{20}$$

$$+(\tfrac{1}{16} - \tfrac{1}{10}s_0 + \tfrac{3}{32}s_0^2 - \tfrac{1}{22}s_0^3 + \tfrac{1}{112}s_0^4)\frac{\tau^6}{30} + \cdots] - aC\tau$$

$$= F(\tau), \tag{D4}$$

with C given by Eq. (D3). Equation (2.19) and Eq. (4.1) yield

$$e^{\tau}\Delta\tilde{G}(\tau) = F(\tau) + \tilde{C}\tau, \tag{D5}$$

where

$$\tilde{C} = \mathrm{P}\int_{s_0}^{\infty} \frac{f(s)ds}{s(s-1)} = (1-b)\ln\frac{s_0}{1-s_0} + \frac{b}{s_0} + \left[\ln\frac{(1+s_0^{-1/3}+s_0^{-2/3})^{1/2}}{s_0^{-1/3}-1}\right.$$

$$\left. + \sqrt{3}\tan^{-1}\frac{\sqrt{3}\,s_0^{-1/3}}{2+s_0^{-1/3}} + 3s_0^{-1/3}\right]a. \tag{D6}$$

For $a = 0.68$, $b = 0.14$ and $s_0 = 0.65$, this function has been plotted in Fig. 5 and as the lower solid curve in Fig. 4.

APPENDIX E: SPECTRAL FUNCTION TEMPERATURE DEPENDENCE

The three-term spectral function at a finite correlation length is calculated in this appendix from a high frequency expansion of the diffusion coefficient. The temperature-dependent generalizations of Eqs. (3.15), (3.16), and (3.17) have been given in Appendix A. The generalization of Eq. (3.25) reads

$$\tilde{\Gamma}(k,\Omega) = \ln(-i\Omega) - \langle \ln\{p^3 + A^{-1}p'^3[1+\eta_1(\kappa^2/p'^2)]\}\rangle$$

$$+\left\langle \ln\left(1 + \frac{p^3 + A^{-1}p'^3[1+\eta_1(\kappa^2/p'^2)]}{-i\Omega}\right)\right\rangle \tag{E1}$$

To obtain the high-frequency expansion for the last term in Eq. (E1), we proceed exactly as in Sec. III. The term in $(-i\Omega)^{-1/3}$ is changed only by the normalization factor I. The coefficient of $\ln(-i\Omega)/(-i\Omega)$ acquires additional κ dependence coming from the expansion of $(p^2+\kappa^2)^{-1}$ and the argument of the loga-

rithm. Thus,

$$\tilde{\Gamma}(\kappa,\Omega)=\ln(-i\Omega)-\langle\ln\{p^3+A^{-1}p'^3[1+\eta_1(\kappa^2p'^2)]\}\rangle+\frac{4\pi\bar{I}^{-1}}{3\sqrt{3}}\left(\frac{(1+A^{-1})}{-i\Omega}\right)^{1/3}+\frac{2\bar{I}^{-1}}{45}(2-A^{-1})\frac{\ln(-i\Omega)}{-i\Omega}$$

$$+\frac{\kappa^2\bar{I}^{-1}}{-i\Omega}\left(\frac{\eta_1A^{-1}}{4\pi}\int\frac{d^3p}{p^2}\frac{p\sin^2\theta'}{p^2}-\frac{1+A^{-1}}{4\pi}\int\frac{d^3p}{p^4}\frac{p^2\sin^2\theta'}{p^2}\right)+\cdots$$

$$=\ln(-i\Omega)-\langle\ln\{p^3+A^{-1}p'^3[1+\eta_1(\kappa^2/p'^2)]\}\rangle+\frac{4\pi\bar{I}^{-1}}{3\sqrt{3}}\left(\frac{1+A^{-1}}{-i\Omega}\right)^{1/3}+\frac{2\bar{I}^{-1}}{45}(2-A^{-1})\frac{\ln(-i\Omega)}{-i\Omega}$$

$$+\frac{2\bar{I}^{-1}}{9}\kappa^2[A^{-1}\eta_1-(1+A^{-1})]\frac{\ln(-i\Omega)}{-i\Omega}+\cdots. \tag{E2}$$

The κ-dependent spectral function consequently is

$$f(s)=1-\frac{2\bar{I}^{-1}}{3}\frac{(1+A^{-1})^{1/3}}{s^{1/3}}-\frac{\bar{I}^{-1}}{s}\left\{\tfrac{2}{45}(2-A^{-1})+\tfrac{2}{9}\kappa^2[A^{-1}\eta_1-(1+A^{-1})]\right\}. \tag{E3}$$

[1]P. C. Hohenberg, E. D. Siggia, and B. I. Halperin, Phys. Rev. B 14, 2865 (1976).

[2]R. A. Ferrell and J. K. Bhattacharjee, Phys. Rev. B 20, 3690 (1979).

[3]V. Dohm, Z. Phys. B31, 327 (1978).

[4]R. Freedman and G. Mazenko, Phys. Rev. B 13, 4967 (1976).

[5]V. Dohm, Solid State Commun. 20, 659 (1976); see also M. Nolan and G. Mazenko, Phys. Rev. B 15, 4077 (1977); J. K. Bhattacharjee and R. A. Ferrell, University of Maryland Technical Report No. 80-030 (unpublished).

[6]H. Burstyn, R. F. Chang, and J. V. Sengers, Phys. Rev. Lett. 44, 410 (1980).

[7]T. Ohta and K. Kawasaki, Prog. Theor. Phys. 55, 1384 (1976).

[8]Yet another approximation to the spectral function can be found in J. K. Bhattacharjee and R. A. Ferrell, University of Maryland Technical Report No. 80-020 (unpublished).

[9]L. S. Ornstein and F. Zernike, Proc. Acad. Sci. Amsterdam 17, 793 (1914); Z. Phys. 19, 134 (1918); 27, 761 (1926). For a further discussion see M. E. Fisher, J. Math. Phys. 5, 944 (1964).

[10]R. A. Ferrell and J. K. Bhattacharjee, Phys. Rev. Lett. 42, 1505 (1979).

[11]R. F. Chang, H. Burstyn, J. V. Sengers, and A. J. Bray, Phys. Rev. Lett. 37, 1481 (1976); R. F. Chang, H. Burstyn, and J. V. Sengers, Phys. Rev. A 19, 866 (1979).

[12]R. A. Ferrell, Phys. Rev. Lett. 24, 1169 (1970).

[13]R. Kubo, J. Phys. Soc. Jpn. 12, 570 (1957); see also M. S. Green, J. Chem. Phys. 22, 398 (1954).

[14]R. Zwanzig, Annu. Rev. Phys. Chem. 16, 67 (1965).

[15]E. D. Siggia, B. I. Halperin, and P. C. Hohenberg, Phys. Rev. B 13, 2110 (1976).

[16]R. Perl and R. A. Ferrell, Phys. Rev. A 6, 2358 (1972); see also Phys. Rev. Lett. 29, 51 (1972).

[17]J. K. Bhattacharjee and R. A. Ferrell, Kinam 2, 63 (1980).

[18]H. C. Burstyn and J. V. Sengers, Phys. Rev. Lett. 45, 259 (1980).

[19]T. Ohta, Kyushu University (unpublished). We thank Dr. Ohta for the communication of his work prior to publication. Ohta's Fig. 2 compares his results with an earlier calculation of this effect by the authors (Ref. 8). The differing specification of the linear term in our earlier work doss not affect the curvature of the semilog plot. Therefore, the discrepancy reported by Ohta is only apparent and not essential.

[20]J. K. Battacharjee and R. A. Ferrell, Phys. Lett. 76A, 290 (1980).

[21]L. Bruschi and M. Santini, Phys. Lett. 73A, 395 (1979); see also A. M. Borghesani, Ph.D. thesis, University of Padua, 1978 (unpublished).